

1 **Extensive profiling of histidine-containing dipeptides reveals species- and tissue-specific distribution**
2 **and metabolism in mice, rats and humans**

3 Thibaux Van der Stede^{1,2,†}, Jan Spaas^{1,3,4,†}, Sarah de Jager^{1,†}, Jana De Brandt^{4,5}, Camilla Hansen², Jan
4 Stautemas¹, Bjarne Vercammen¹, Siegrid De Baere⁶, Siska Croubels⁶, Charles-Henri Van Assche⁷, Berta
5 Cillero Pastor⁷, Michiel Vandenbosch⁷, Ruud Van Thienen¹, Kenneth Verboven^{4,5}, Dominique
6 Hansen^{4,5,8}, Thierry Bové⁹, Bruno Lapauw¹⁰, Charles Van Praet^{11,12}, Karel Decaestecker^{11,12}, Bart
7 Vanaudenaerde¹³, Bert O Eijnde^{3,14,15}, Lasse Gliemann², Ylva Hellsten², Wim Derave^{1,*}

8 ¹ Department of Movement and Sports Sciences, Ghent University, Belgium.

9 ² Department of Nutrition, Exercise and Sports, Copenhagen University, Denmark.

10 ³ University MS Center (UMSC) Hasselt – Pelt, Belgium.

11 ⁴ BIOMED Biomedical Research Institute, Hasselt University, Belgium.

12 ⁵ REVAL Rehabilitation Research Center, Hasselt University, Belgium.

13 ⁶ Department of Pathobiology, Pharmacology and Zoological Medicine, Ghent University, Belgium.

14 ⁷ The Maastricht MultiModal Molecular Imaging (M4I) institute, Maastricht University, The
15 Netherlands

16 ⁸ Heart Center Hasselt, Jessa Hospital Hasselt, Belgium.

17 ⁹ Department of Cardiac Surgery, Ghent University Hospital, Belgium.

18 ¹⁰ Department of Endocrinology, Ghent University Hospital, Belgium.

19 ¹¹ Department of Urology, Ghent University Hospital, Belgium.

20 ¹² Department of Human Structure and Repair, Ghent University, Belgium.

21 ¹³ Department of Chronic Diseases and Metabolism, KU Leuven, Belgium.

22 ¹⁴ SMRC Sports Medical Research Center, BIOMED Biomedical Research Institute, Hasselt University,
23 Belgium.

24 ¹⁵ Division of Sport Science, Stellenbosch University, South Africa.

25

26 [†] These authors have contributed equally

27 * Correspondence: Wim.Derave@UGent.be (Watersportlaan 2, 9000 Gent, Belgium)

28 This manuscript has been uploaded to a preprint server (BiorXiv, CC-BY-NC-ND 4.0 International
29 license).

30

31 Classification:

32 Major (Biological sciences)

33 Minor (Physiology)

34 Abstract

35 Histidine-containing dipeptides (HCDs) are pleiotropic homeostatic molecules linked to inflammatory,
36 metabolic and neurological diseases, as well as exercise performance. Using a sensitive UHPLC-MS/MS
37 approach and an optimized quantification method, we performed a systematic and extensive profiling
38 of HCDs in the mouse, rat, and human body (in n=26, n=25, n=19 tissues, respectively). Our data show
39 that tissue HCD levels are uniquely regulated by carnosine synthase (CARNS1), an enzyme that was
40 preferentially expressed by fast-twitch skeletal muscle fibers and brain oligodendrocytes. Cardiac HCD
41 levels are remarkably low compared to other excitable tissues. Carnosine is unstable in human plasma,
42 but is preferentially transported within red blood cells in humans but not rodents. The low abundant
43 carnosine analog N-acetylcarnosine is the most stable plasma HCD, and is enriched in human skeletal
44 muscles. Here, N-acetylcarnosine is continuously secreted into the circulation, which is further induced
45 by acute exercise in a myokine-like fashion. Collectively, we provide a novel basis to unravel tissue-
46 specific, paracrine, and endocrine roles of HCDs in human health and disease.

47

48 **Key words:** histidine-containing dipeptides, central nervous system, muscle, exercise

49

50 **Significance statement:** By extensively profiling the pluripotent histidine-containing dipeptides across
51 three species, we generated many new insights into species- and tissue-specific histidine-containing
52 dipeptide metabolism. For instance, the only stable analog that is specific for the human circulation
53 (N-acetylcarnosine) is continuously released from muscle tissue and is positively regulated by physical
54 exercise. The great number of analyses and experiments involving humans establishes great
55 translational value of the findings. These new data open exciting opportunities to study histidine-
56 containing dipeptide metabolism, including paracrine and/or endocrine signaling of these dipeptides,
57 possibly contributing to the potent health-promoting exercise effects.

58 Introduction

59 Carnosine synthase (CARNS1) is presumably the only enzyme in animals capable of synthesizing an
60 abundant class of endogenous dipeptides. The enzyme links L-histidine to either β -alanine or γ -
61 aminobutyric acid (GABA), respectively rendering carnosine or homocarnosine. These parent
62 dipeptides and their methylated (anserine and balenine) and acetylated (N-acetylcarnosine) analogs
63 are collectively called the histidine-containing dipeptides (HCDs).

64 Since the initial discovery in 1900 by Vladimir Gulevich (1), carnosine and the other HCDs have been
65 linked to various physiological functions, mostly serving to preserve redox status and cellular
66 homeostasis (for a full overview, see (2)). The most relevant biochemical properties for their functions
67 relate to proton buffering, metal chelation and antioxidant capacity, which further translates to
68 protection against advanced glycation and lipoxidation end products (3, 4). The physiological
69 importance of tissue HCD content is underscored by an extensive body of research ranging from
70 enhancement of exercise performance (5) to treatment of cardiometabolic (6, 7) or neurological
71 diseases (8) in rodents. Major differences between animal and human HCD metabolism may be present
72 however, given that high carnosinase (CN1) activity in human, but not rodent, plasma results in rapid
73 degradation of carnosine (9, 10).

74 Nevertheless, even more than 120 years after the initial discovery of carnosine and 10 years after the
75 molecular identification of CARNS1 (11), there remains a lack of basic understanding of HCD synthesis,
76 distribution, and metabolism throughout the animal and especially the human body. It is thought that
77 HCDs are primarily expressed in excitable tissues such as skeletal and cardiac muscle and the central
78 nervous system (CNS), but current literature mostly consists of scattered observations focussing on a
79 limited number of tissues or species. Information on cardiac levels is sparse, although HCDs could play
80 an important role in cardiomyocyte homeostasis (12). Furthermore, there is unclarity regarding the
81 synthesis and physiological role of HCDs in kidney, lung, liver, and other non-excitable tissues. A first
82 profiling of HCDs in rat tissues from Aldini *et al.* (13) did not detect HCDs in non-excitable tissues,
83 although this and other previous endeavours were potentially limited from lower detection sensitivity
84 compared to the currently available technology. For example, the low abundant HCDs anserine,
85 balenine and N-acetylcarnosine have never been extensively characterized in animal or human tissues.

86 Here, we have performed the first systematic profiling of the five main HCDs, combined with
87 determination of CARNS1 expression levels, in the mouse, rat and human body. Various human tissue
88 samples were collected from live donors, except for post-mortem collected brain regions. We
89 uncovered profound differences in HCD distribution and metabolism between tissues and species. For

90 instance, we demonstrate that humans have a unique way of circulating HCDs and releasing it from
91 carnosine-synthesizing tissues such as skeletal muscle.

92 Results

93 CARNS1 is the unique and rate-limiting enzyme for HCD synthesis

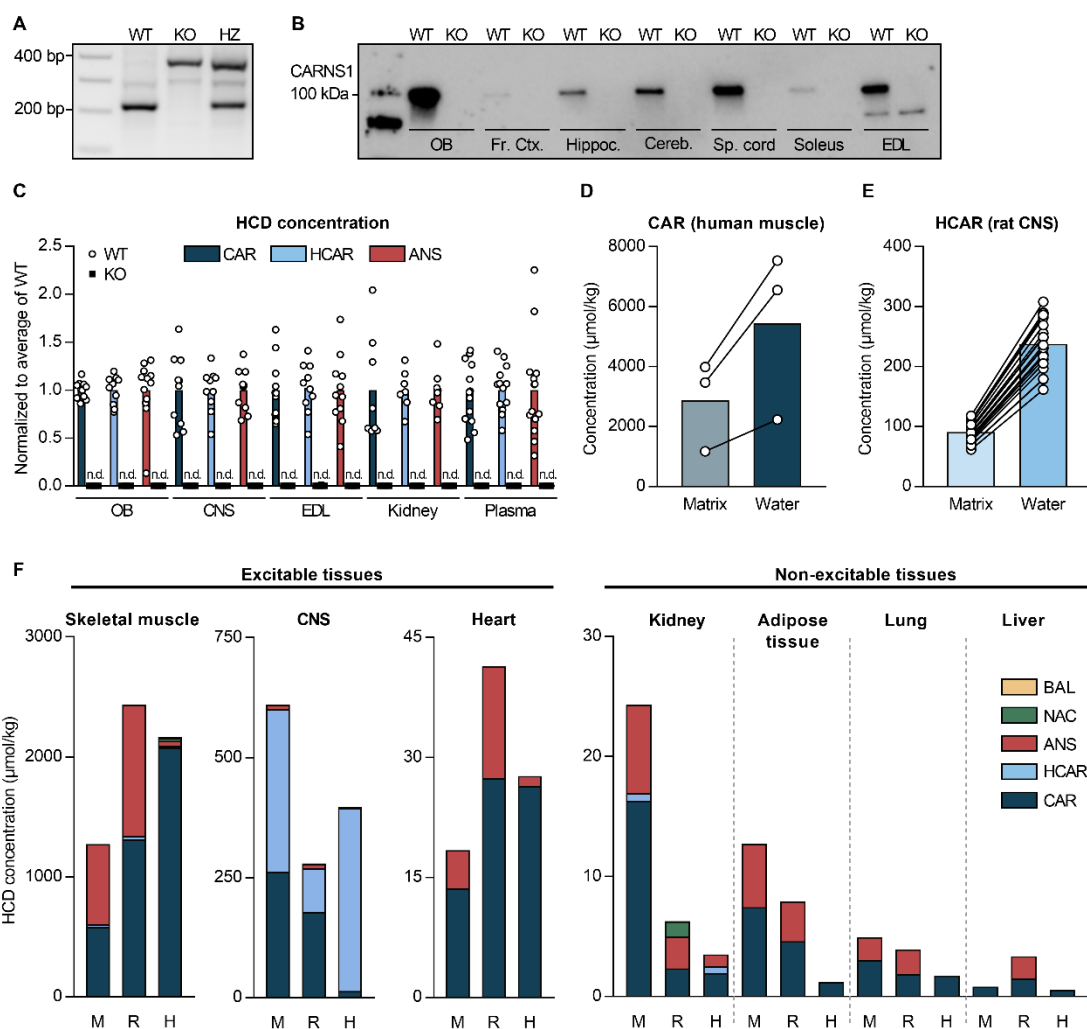
94 Using whole-body *Carns1*-knockout (KO) mice, we aimed to investigate whether CARNS1 deficiency
95 results in a complete lack of endogenous (homo)carnosine and their derivatives in a variety of tissues,
96 which would imply that CARNS1 is the unique and rate-limiting enzyme for HCD synthesis. CARNS1 was
97 successfully knocked out at the gene (**Fig 1A**) and protein (100 kDa, **Fig 1B**) level, thereby also validating
98 our Western blot antibody for specifically detecting the CARNS1 protein. As described previously,
99 *Carns1*-KO mice displayed normal growth and survival (14). The deletion of *Carns1* led to an absence
100 of carnosine and homocarnosine in all investigated tissues (**Fig 1C**). Similarly, these mice were devoid
101 of the carnosine-derived analogs anserine, balenine and N-acetylcarnosine (of which only anserine is
102 consistently present in mouse tissues, cfr. infra, **Fig 1C**).

103 In addition, tissue from *Carns1*-KO mice was used to optimise our quantitative UHPLC-MS/MS-based
104 detection of HCDs. Concentration levels in muscle and brain were compared using matrix-matched
105 standard calibration curve preparation in *Carns1*-KO tissue matrix (i.e. muscle or brain homogenates)
106 and water (as current standard practice in HCD research). In water, HCD levels were overestimated by
107 ~2 to 3-fold (**Fig 1D-E**), indicating the importance of utilizing a corresponding blank tissue matrix for
108 HCD quantification. This approach was used for all further analyses in this paper (except human
109 cerebrospinal fluid), rendering the HCD quantifications more accurate than previously reported.

110

111 HCDs are not excitable tissue-specific metabolites

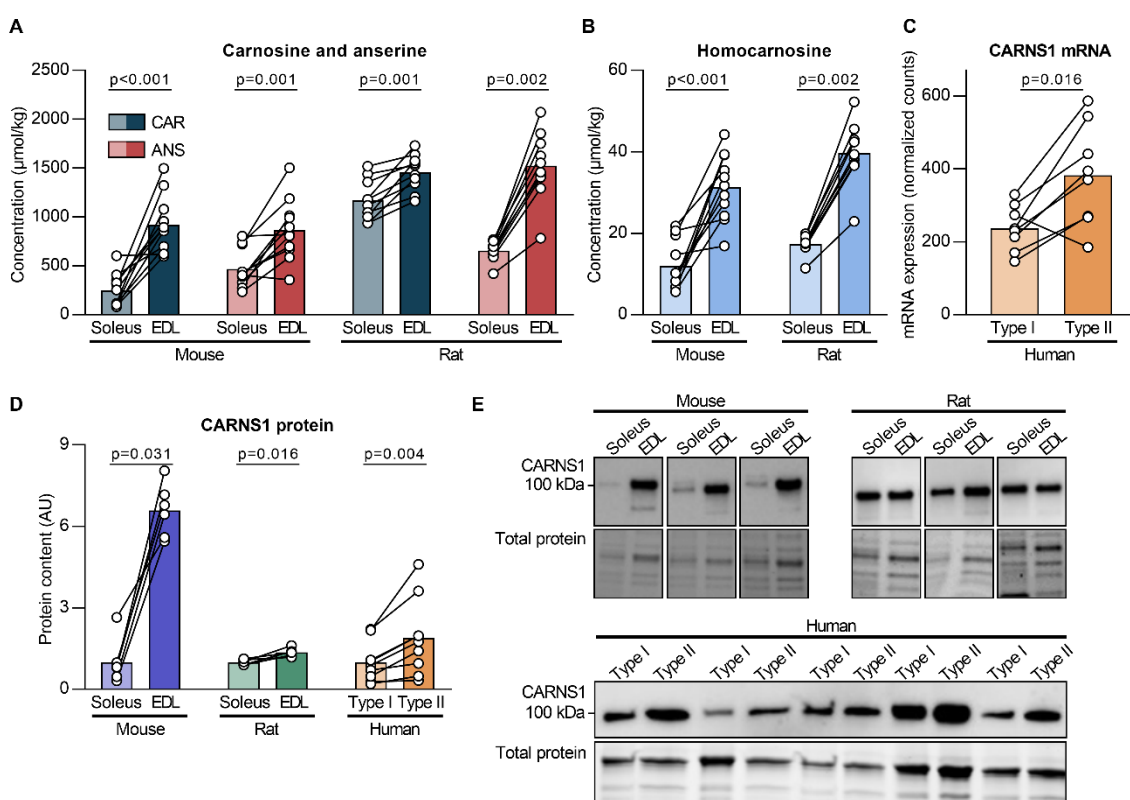
112 Using our sensitive UHPLC-MS/MS method, we performed a systematic profiling of HCDs in various
113 tissues of the mouse, rat, and human body (**Fig 1F**, **Table S1**). Carnosine was the only HCD present in
114 all studied tissues across the three species. Skeletal muscles contained the largest amounts of HCDs,
115 followed by the CNS, up to the millimolar range. However, not all excitable tissue contained large
116 amounts of HCDs, since unexpectedly low HCD levels were observed in the heart of all three species
117 (50-100 times lower than skeletal muscles). These low HCD levels in cardiac tissue better reflect those
118 measured in non-excitable tissues. Besides skeletal muscle, CNS, heart, kidney, adipose, lung and liver
119 tissue (presented in **Fig 1F**), we also found low levels of HCDs in the mouse and rat stomach wall,
120 gallbladder, pancreas, small intestine, colon, thymus, spleen, and eye (**Table S1**).



121
122 **Figure 1. Species- and tissue-specific distribution of histidine-containing dipeptides.** (A) PCR gel and (B) Western blot
123 showing the successful knockout of the *Carns1* gene and the absence of CARNS1 protein in mice. (C) HCD measurements
124 by UHPLC-MS/MS showing HCDs are absent from various tissues of *Carns1*-KO compared to WT mice. (D) Carnosine and
125 (E) homocarnosine measured by UHPLC-MS/MS, followed by quantification based on a standard calibration curve
126 prepared in water vs. *Carns1*-KO tissue matrix. (F) HCD measurements by UHPLC-MS/MS in skeletal muscle, CNS, heart,
127 kidney, adipose tissue, lung, and liver tissue from mice (M), rats (R) and humans (H). Values were averaged if more than
128 1 type of the respective tissue was present (e.g. soleus and EDL for rodent muscle). ANS, anserine; BAL, balenine; CAR,
129 carnosine; Cereb., cerebellum; CNS, central nervous system; EDL, extensor digitorum longus; Fr. ctx., frontal cortex;
130 HCAR, homocarnosine; Hippoc., hippocampus; HZ, heterozygous; KO, knockout; NAC, N-acetylcarnosine; OB, olfactory
131 bulb; Sp. cord, spinal cord; WT, wild type.

132
133 CARNS1 content drives fiber type-related differences in HCD content in skeletal muscle
134 We next aimed to profile the HCD content in skeletal muscle in more detail, with a focus on potential
135 fiber type-specific differences. In mice and rats, we determined the HCD content in soleus (more
136 oxidative, slow-twitch) and extensor digitorum longus (EDL; more glycolytic, fast-twitch) muscles. Our
137 results confirmed previous reports (15-17) that carnosine and anserine content is higher in EDL muscle
138 (**Fig 2A**). Also the homocarnosine content was ~2.5-fold higher in EDL compared to soleus in both mice
139 and rats (**Fig 2B**). To get more insights if CARNS1 content (i.e. HCD production) is the main driver for

140 the fiber type-related differences, we first explored a publicly available human muscle fiber type-
141 specific RNAseq dataset (18). These data show a ~2-fold higher *CARNS1* mRNA content in type IIa vs.
142 type I fibers (Fig 2C). We next determined *CARNS1* protein levels in the soleus and EDL muscles from
143 the mice and rats (Fig 2D-E). *CARNS1* levels were indeed higher in EDL muscles, with a larger difference
144 between soleus and EDL muscles in mice (6.6-fold) than in rats (1.4-fold). To translate mRNA
145 differences in human muscle to the protein level, we used Western blotting on pools of pre-classified
146 type I or type IIa fibers (Fig S1). This revealed a ~2-fold higher *CARNS1* content in type IIa fibers (Fig
147 2D-E), consistent with findings at the mRNA level. These results suggest that *CARNS1* expression is the
148 main driver regulating the clear fiber type-related differences in HCD content across the three species.



149

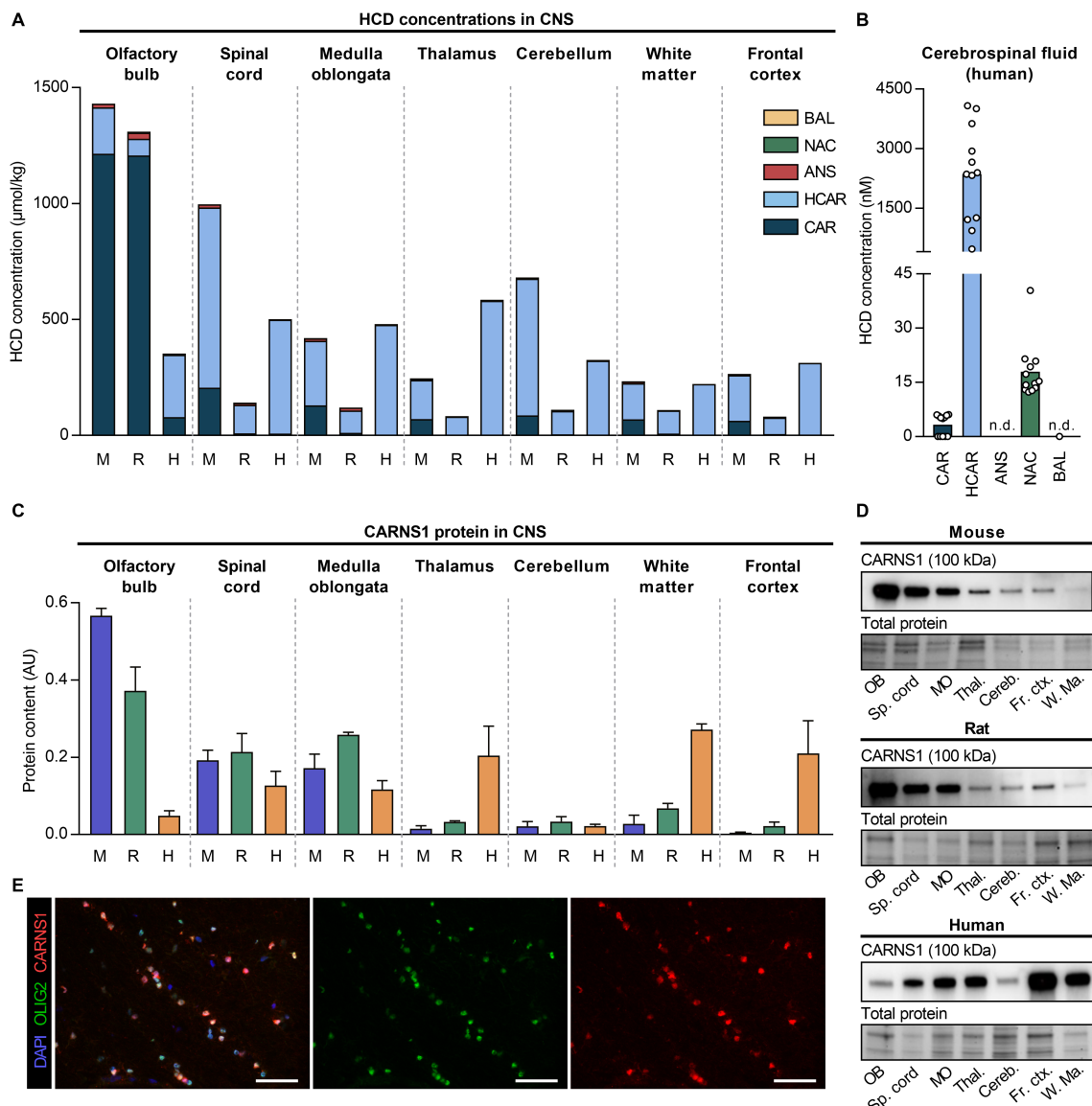
150 **Figure 2. Muscle and muscle fiber type-specific differences in histidine-containing dipeptides and *CARNS1*.** (A)
151 Carnosine and anserine and (B) measurements by UHPLC-MS/MS in soleus and EDL muscles from mice and rats. (C)
152 Human muscle fiber type-specific calculation of *CARNS1* mRNA based on a previously published dataset. (D) Protein
153 levels of *CARNS1* determined by Western blot in soleus and EDL muscle from mice and rats, and human type I and type
154 II fiber pools. (E) Representative Western blot and loading controls. ANS, anserine; CAR, carnosine; EDL, extensor
155 digitorum longus.

156

157 Homocarnosine is the dominant HCD in the CNS, except for the olfactory bulb of rodents

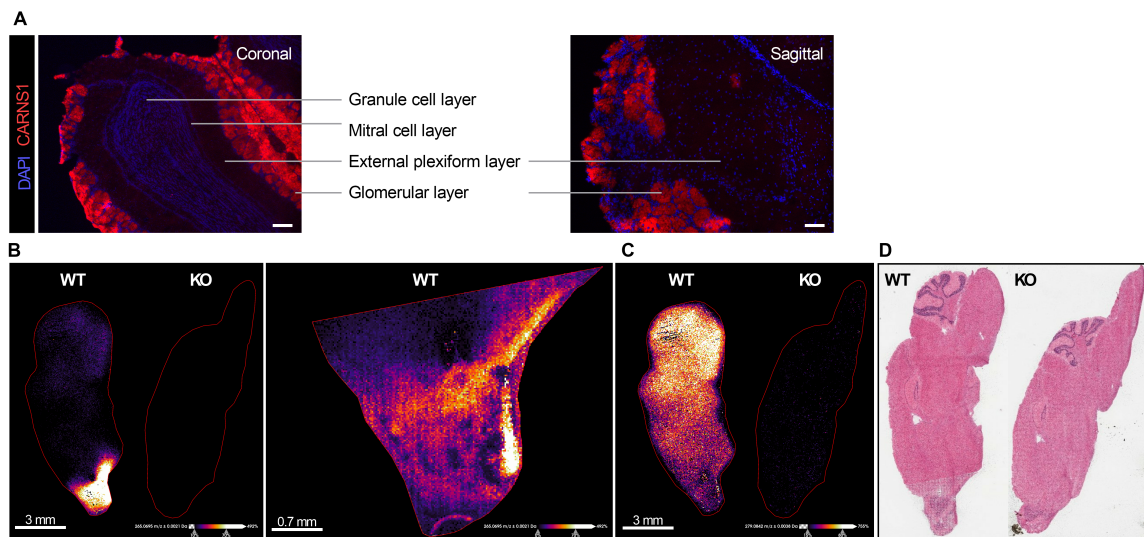
158 Apart from skeletal muscle, HCDs are also highly present in the CNS. By analyzing seven different
159 regions from the mouse, rat and human CNS, we could confirm that the highest levels of carnosine are
160 found in the olfactory bulb in rodents, reaching concentrations of ~1200 μ mol/kg tissue, which is

161 similar to or even higher than skeletal muscle carnosine levels (**Fig 3A, Table S1**). In contrast, the
162 human olfactory bulb contained approximately 15 times less carnosine (~80 μ mol/kg). In mice and
163 rats, the olfactory bulb was the only CNS region containing more carnosine than homocarnosine, whilst
164 in humans all regions contained more homocarnosine than carnosine. Similar to our findings in human
165 CNS tissue, homocarnosine was also abundantly present in human cerebrospinal fluid (**Fig 3B**).
166 CARNS1 protein levels also showed considerable variability between CNS regions (**Fig 3C-D**). Mice and
167 rats exhibited high expression in olfactory bulb, as well as the spinal cord and medulla oblongata, but
168 not the rest of the CNS. In human tissues, we found lower CARNS1 levels in the olfactory bulb, but
169 instead observed greater amounts in the white matter, thalamus, and frontal cortex.
170 Immunofluorescence was used to further study the localisation of CARNS1 in the CNS. We chose the
171 region exhibiting the greatest CARNS1 protein levels among rodents (mouse olfactory bulb) and
172 humans (white matter). Double-labeling of CARNS1 and OLIG2, an oligodendrocyte lineage marker,
173 revealed that CARNS1 resides in oligodendrocytes of human white matter (**Fig 3E**). Cell markers for
174 microglia (CD68, **Fig S2A**), astrocytes (GFAP, **Fig S2B**) and neurons/axons (NF-H, **Fig S2C**) did not co-
175 localise with CARNS1. In the mouse olfactory bulb, CARNS1 appeared in spherical structures near the
176 surface of the olfactory bulb, i.e. the glomeruli, where olfactory nerve terminals form synapses with
177 dendrites from projection neurons that carry signals into the brain (**Fig 4A**). A similar spatial
178 distribution was present for carnosine, as mass spectrometry imaging detected higher levels at the
179 border compared to the center of the mouse olfactory bulb (**Fig 4B**). In contrast, homocarnosine
180 displayed a more dispersed distribution throughout the mouse CNS, as well as an overall anterior-to-
181 posterior gradient with greater amounts of homocarnosine in the midbrain, hindbrain, cerebellum,
182 and spinal cord (**Fig 4C**). As expected, (homo)carnosine could not be detected in *Carns1*-KO mice (**Fig**
183 **4B-D**).



184

185 **Figure 3. Region-specific levels of histidine-containing dipeptides and CARNS1 in the mouse, rat and human central**
 186 **nervous system. (A) HCD measurements by UHPLC-MS/MS in seven different central nervous system regions from mice**
 187 **(M), rats (R) and humans (H). (B) HCD measurements by UHPLC-MS/MS in human cerebrospinal fluid.** (C) Protein levels
 188 **of CARNS1 determined by Western blot in seven different central nervous system regions from mice, rats and humans.**
 189 **Data are mean \pm SD. (D) Representative Western blot and loading controls. (E) Immunohistochemical detection of**
 190 **CARNS1 and OLIG2 in human white matter. In panels (A), (C) and (D), spinal cord tissue is from the cervical region, mouse**
 191 **white matter is from the corpus callosum, and human frontal cortex is from the superior frontal gyrus. ANS, anserine;**
 192 **AU, arbitrary units; BAL, balenine; CAR, carnosine; Cereb., cerebellum; CNS, central nervous system; Fr. ctx., frontal**
 193 **cortex; HCAR, homocarnosine; MO, medulla oblongata; NAC, N-acetylcarnosine; OB, olfactory bulb; Sp. cord, spinal cord;**
 194 **Thal., thalamus; W. Ma., white matter. Scale bars are 50 μ m (E).**



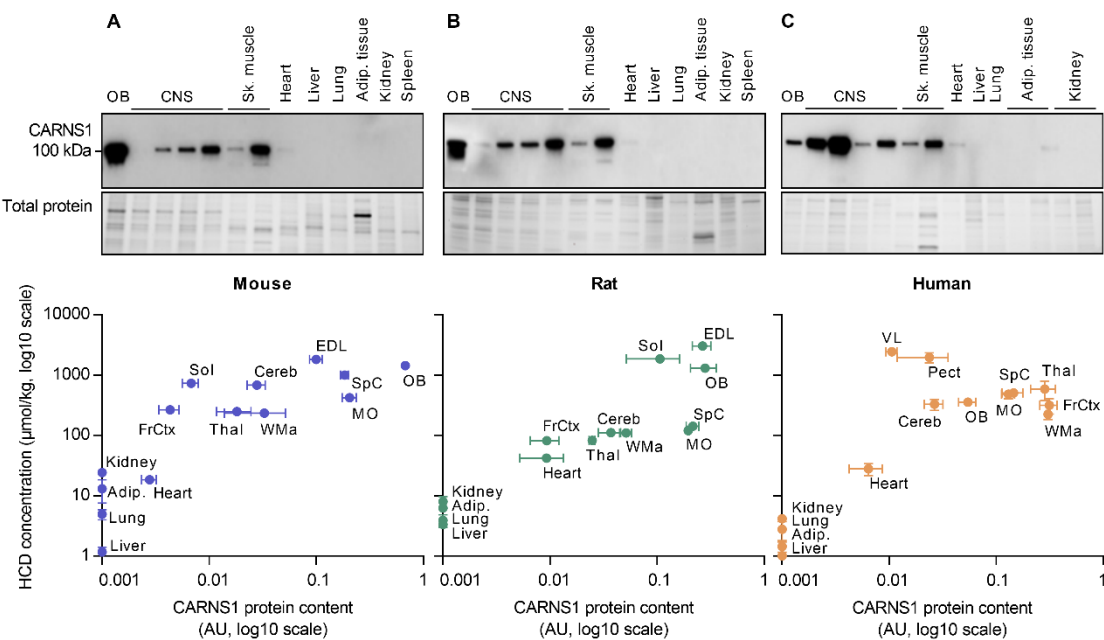
195

196 **Figure 4. Spatial localisation of CARNS1 and (homo)carnosine within the mouse central nervous system.** (A)
197 Immunohistochemical detection of CARNS1 in mouse olfactory bulb. Scale bars are 100 µm. (B) Mass spectrometry
198 imaging (MALDI-MSI) of carnosine in whole mouse brain (50 µm spatial resolution) or olfactory bulb only (20 µm spatial
199 resolution). WT and *Carns1*-KO mouse. (C) Mass spectrometry imaging (MALDI-MSI) of homocarnosine in whole mouse
200 brain (50 µm spatial resolution). WT and *Carns1*-KO mouse. (D) H&E staining of the representative WT and *Carns1*-KO
201 mouse brains. KO, knockout; WT, wild type.

202

203 CARNS1 expression scales with tissue HCD levels on a whole-body level

204 To investigate if tissue CARNS1 expression closely relates to tissue HCD levels, CARNS1 protein levels
205 (Western blot) were plotted against HCD concentrations (UHPLC-MS/MS). If the tissue CARNS1 level is
206 the main determinant of tissue HCD levels, a linear relation between both variables is expected. In all
207 non-excitable tissues, no CARNS1 could be detected by Western blot (Fig 5A-C). HCD levels in these
208 tissues probably reflect transmembrane HCD uptake. On a whole-body level, CARNS1 scaled with HCD
209 levels in mice (Fig 5A), rats (Fig 5B) and humans (Fig 5C). However, when comparing within organs,
210 more CARNS1 was not always directly linked to a higher HCD concentration. In the human CNS, for
211 example, CARNS1 was 13-fold higher in white matter than in the cerebellum, but both tissues had
212 similar HCD levels. This indicates that although CARNS1 is the only enzyme responsible for HCD
213 synthesis, other factors, such as exchange of HCDs between organs or a high HCD turnover rate
214 (synthesis/degradation), could also influence intracellular HCD levels.



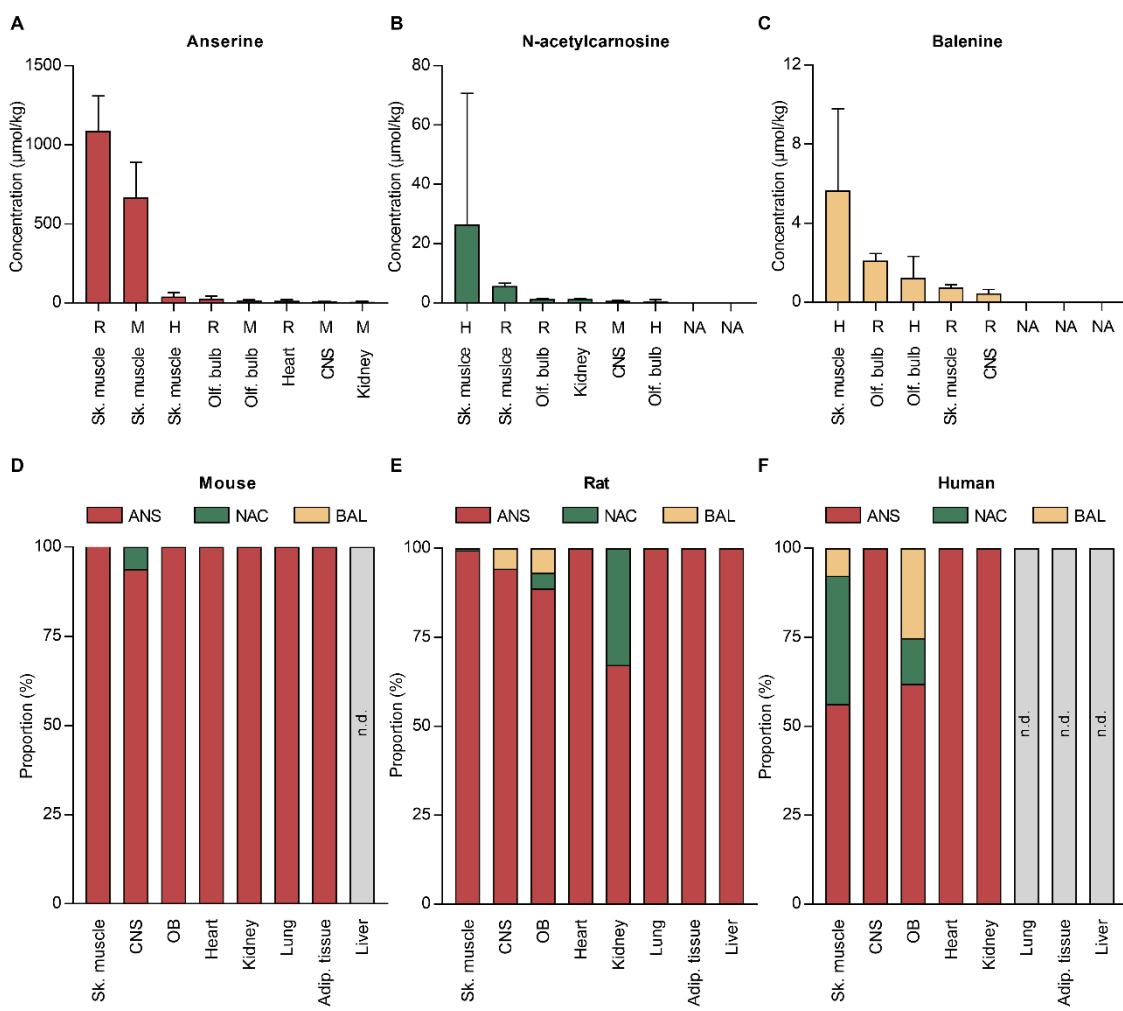
215

216 **Figure 5. Association between CARNS1 and tissue histidine-containing dipeptide levels.** Plotted relationship between
217 CARNS1 levels (Western blot) and HCD measurements (UHPLC-MS/MS) in a variety of (A) mouse, (B) rat, and (C) human
218 tissues. The central nervous system (CNS) regions that are shown, besides the olfactory bulb (OB), are frontal cortex
219 (FrCtx), cerebellum (Cereb), spinal cord (SpC), thalamus (Thal), white matter (WMA) and medulla oblongata (MO). Mouse
220 muscles are soleus (Sol) and extensor digitorum longus (EDL). Human muscles are m. vastus lateralis (VL) and m.
221 pectoralis (Pect). Human adipose tissue is subcutaneous and visceral fat (Adip). Human kidney is medulla and cortex.
222 Data are mean \pm SEM. AU, arbitrary units.

223

224 N-acetylcarnosine and balenine are mainly found in human skeletal muscle

225 Whilst the parent HCDs (carnosine and homocarnosine) were ubiquitously expressed, most of the
226 examined tissues also contained at least one methylated (anserine or balenine) or acetylated (N-
227 acetylcarnosine) carnosine analog (Fig 1F). Rodent skeletal muscles contained by far the highest
228 anserine levels (up to \sim 1500 μ mol/kg in the rat EDL, Fig 6A). Besides anserine (\sim 40 μ mol/kg, Fig 6A),
229 human skeletal muscle also contained N-acetylcarnosine (\sim 25 μ mol/kg, Fig 6B) and balenine (\sim 5
230 μ mol/kg, Fig 6C). In fact, human skeletal muscle was the tissue where we observed the highest N-
231 acetylcarnosine and balenine levels. Fig 6D-F display the proportion of methylated or acetylated
232 carnosine variants in different species and tissues.



233

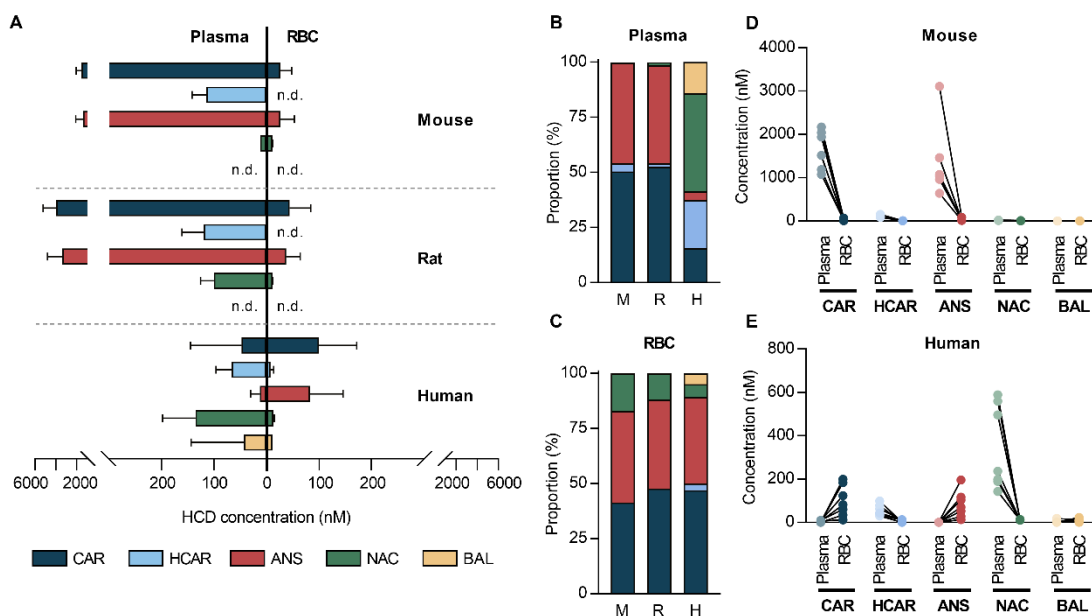
234 **Figure 6. Anserine, N-acetylcarnosine and balenine levels in mouse, rat and human tissues. (A) Anserine, (B) N-**
235 **acetylcarnosine, and (C) balenine measurements by UHPLC-MS/MS in mouse (M), rat (R), and human (H) tissues. The**
236 **figures display the 8 tissues with the highest concentration of each dipeptide. Data are mean \pm SD. (D-F) Relative**
237 **proportion of anserine, N-acetylcarnosine, and balenine in (D) mouse, (E) rat, and (F) human tissues. Adip., adipose;**
238 **ANS, anserine; BAL, balenine; CNS, central nervous system; NAC, N-acetylcarnosine; n.d., not detectable; Olf. bulb,**
239 **Sk., skeletal.**

240

241 Acetylation of carnosine provides stability in the human circulation, which is not required in red blood
242 cells or rodents

243 Since rodents and humans differ substantially in presence and activity of the hydrolyzing enzyme CN1
244 in the circulation (2, 10), we attempted to map the circulating content of the five main HCDs. As
245 expected, levels of plasma carnosine and anserine were very high in mice (~ 1500 nM) and rats (~ 3500
246 nM), but in the low nanomolar range in humans (Fig 7A). Low levels of homocarnosine could be
247 detected in all 3 species, while balenine was only present in human plasma (Fig 7A). Interestingly, N-
248 acetylcarnosine was the most abundant HCD in the human circulation, accounting for $\sim 45\%$ of the total
249 HCDs (Fig 7B). Although HCD levels in red blood cells (RBCs) were in the nanomolar range in all 3
250 species, striking differences were observed compared to plasma (Fig 7A and 7C). For both rodent

251 species, HCD levels were drastically lower in RBCs than plasma (**Fig 7D** and **S3**). On the contrary, human
252 carnosine and anserine levels were higher in every RBC sample compared to plasma, whilst N-
253 acetylcarnosine levels were lower in RBCs than plasma (**Fig 7E**). These data suggest that carnosine in
254 the human circulation is rendered more stable via acetylation to N-acetylcarnosine (which is resistant
255 to hydrolysis by CN1) or via transport inside RBCs.



256
257 **Figure 7. Species differences in histidine-containing dipeptides in plasma and red blood cells.** (A) HCD measurements
258 by UHPLC-MS/MS in mouse, rat and human plasma and red blood cells (data are mean \pm SD). (B) Relative proportion of
259 each HCD in mouse (M), rat (R) and human (H) plasma. (C) Relative proportion of each HCD in mouse, rat and human red
260 blood cells. (D) Direct comparison of HCDs in plasma and red blood cells collected from the same mice. (E) Direct
261 comparison of HCDs in plasma and red blood cells collected from the same human individuals. ANS, anserine; BAL,
262 balenine; CAR, carnosine; HCAR, homocarnosine; NAC, N-acetylcarnosine; RBC, red blood cells.

263
264 Oral β -alanine supplementation affects HCDs in skeletal muscle and circulating N-acetylcarnosine
265 levels in humans

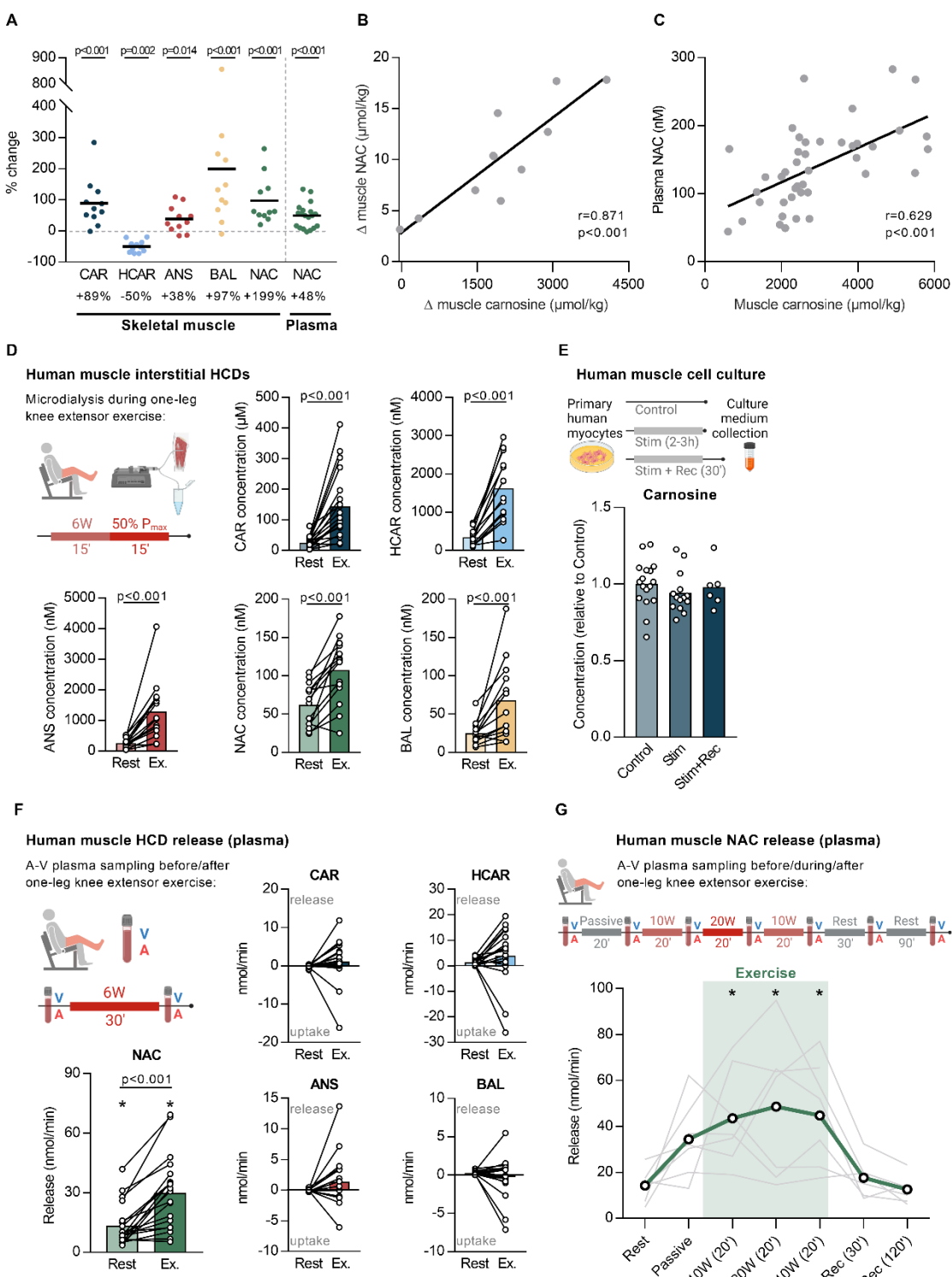
266 We next investigated the effects of chronic supplementation of the rate-limiting precursor β -alanine
267 on the content of all five HCDs in human skeletal muscle. As expected, β -alanine supplementation
268 increased muscle carnosine content (+89%, **Fig 8A** and **S4A**). In addition, we observed increases in
269 muscle anserine (+38%, **Fig 8A** and **S4B**), N-acetylcarnosine (+97%, **Fig 8A** and **S4C**) and balenine
270 (+199%, **Fig 8A** and **S4D**), and these increases were proportional to the carnosine increase (**Fig 8B**).
271 However, homocarnosine content significantly decreased (-50%) after 12 weeks of β -alanine
272 supplementation (**Fig 8A** and **S4E**). Plasma N-acetylcarnosine increased by 48% after the
273 supplementation period (**Fig 8A** and **S4F**), which correlated at the individual level with muscle
274 carnosine content (**Fig 8C**), suggesting a possible link between intramuscular and circulating HCD levels.

275 In summary, oral β -alanine supplementation is a potent stimulus affecting all HCDs in skeletal muscle,
276 and plasma N-acetylcarnosine may reflect muscle HCD levels under baseline conditions and during β -
277 alanine supplementation.

278

279 N-acetylcarnosine is released from human skeletal muscle during exercise

280 Given this likely relationship between intra- and extracellular HCDs, and given that skeletal muscle is
281 the main active organ during exercise, we explored HCD dynamics during exercise. First, we collected
282 muscle interstitial fluid at rest and during exercise in humans. During exercise, interstitial levels for
283 every HCD increased (**Fig 8D**). This increase could however be primarily caused by sarcolemmal
284 damage following insertion of the microdialysis probe (19). To check this, we performed two follow-
285 up experiments. Firstly, *in vitro* human primary muscle cells were electrically stimulated for 2-3 h to
286 simulate muscle contraction. This did not result in secretion of carnosine into the culture medium
287 immediately after the electrical stimulation or following 30 min recovery (**Fig 8E**). Other HCDs could
288 not be detected in the cell culture medium. Secondly, we collected interstitial fluid from mouse skeletal
289 muscle, with a previously published method in which the muscle is not mechanically affected (20, 21).
290 Interstitial levels of carnosine and anserine were not higher in exercised mice compared to control
291 mice (**Fig S5A**). Next, we collected samples of the femoral artery and vein at rest and during exercise
292 (from a group of postmenopausal women). Our results clearly indicate a release of N-acetylcarnosine
293 from muscle tissue at rest of \sim 13 nmol/min (from one leg), which further increased \sim 2-fold during
294 exercise (**Fig 8F**). No release at rest or during exercise was observed for any of the other HCDs (**Fig 8F**).
295 These results were confirmed using a similar experimental setup in healthy young men, and with more
296 sampling time points during rest, passive movement, exercise and recovery. Here, we again showed a
297 release of N-acetylcarnosine at rest (\sim 14 nmol/min from one leg), which increased 3.4-fold during
298 exercise and quickly returned back to baseline during recovery (**Fig 8G**). Exercise did not induce
299 carnosine release or uptake within RBCs (**Fig S5B**). Also in mice, no changes in carnosine or anserine
300 levels within plasma were observed following 60 min exercise (**Fig S5C**). Taken together, these data
301 indicate that N-acetylcarnosine in humans is likely the major, or most stable, HCD released during
302 exercise in a myokine-like fashion.

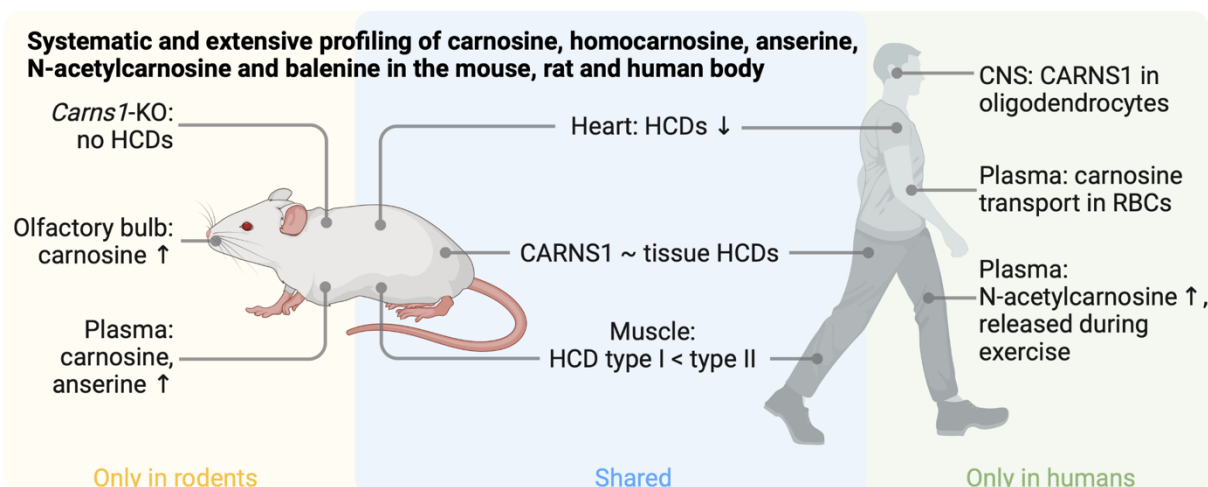


303 **Figure 8. β -alanine supplementation and N-acetylcarnosine release during exercise from human muscle. (A)** Changes
 304 in HCD levels, measured by UHPLC-MS/MS, in human skeletal muscle (m. vastus lateralis) after β -alanine
 305 supplementation. **(B)** Correlation between supplementation-induced changes in skeletal muscle carnosine and N-
 306 acetylcarnosine, measured by UHPLC-MS/MS. **(C)** Correlation between skeletal muscle carnosine and plasma N-
 307 acetylcarnosine, measured by UHPLC-MS/MS. **(D)** HCD measurements by UHPLC-MS/MS in human skeletal muscle
 308 interstitial fluid at rest and following exercise (Ex.). **(E)** Carnosine measurements by UHPLC-MS/MS in culture medium
 309 from primary human muscle cells in control condition, after 2-3 h of electrical stimulation (Stim), and after 2-3 h of
 310 electrical stimulation followed by 30 min recovery (Stim+Rec). **(F)** HCD measurements by UHPLC-MS/MS in human
 311 arterial and venous plasma samples at rest and following exercise (Ex.). Positive values indicate a net release, negative
 312 values indicate a net uptake. Asterisk indicates significantly different from zero release at the respective time point. **(G)**

314 Release of N-acetylcarnosine in human plasma, based on arterio-venous differences, at rest, during passive movement,
315 at different time points during exercise, and up to 120 min recovery (Rec). Positive values indicate a net release, negative
316 values indicate a net uptake. ANS, anserine; A-V; arterio-venous, BAL, balenine; CAR, carnosine; HCAR, homocarnosine;
317 NAC, N-acetylcarnosine.

318 Discussion

319 This is the first study to systematically and extensively profile the organ distribution of HCDs and their
320 differences between mice, rats and humans. Although present in all investigated non-excitable tissues
321 in minute amounts, mainly excitable tissues contained high HCD levels in all species. Yet, our data show
322 surprisingly low values in cardiac tissue across species, and a different distribution of HCDs in CNS
323 regions between species. The enzyme CARNS1 is the unique enzyme responsible for endogenous
324 carnosine and homocarnosine synthesis, and is a major determinant for tissue HCD levels. In human
325 CNS white matter, CARNS1 appears restricted to cells from the oligodendrocyte lineage. We also
326 uncover that N-acetylcarnosine is the primary circulating HCD in human plasma and is continuously
327 secreted from skeletal muscle into the circulation, which is further increased by physical exercise. An
328 overview of the main findings is visualized in **Fig 9**.



329 **Figure 9. Graphical summary.** Visual representation of the main findings, based on our extensive profiling of histidine-
330 containing dipeptides (HCDs) in mice, rats and humans, and related follow-up experiments. Arrow up indicates high
331 abundance, arrow down indicates low abundance. CNS, central nervous system; RBC, red blood cell.

332
333 Previous endeavors to profile HCDs mostly focused on rodent tissues, and resulted in fragmented and
334 sometimes contradictory literature (13, 22-25). Our systematic approach and very sensitive state-of-
335 the-art UHPLC-MS/MS methodology facilitate direct comparison between tissues and species. Our
336 data contradicted some of the previous findings, e.g. that human muscle contains only carnosine and
337 no other HCDs (2), that rat kidney, lung, plasma and liver lack HCDs (13), or that homocarnosine is
338 exclusively found in the CNS (26), with no presence of carnosine in the human brain or cerebrospinal
339 fluid (27). We confirmed that anserine is predominantly found in rodent skeletal muscles (2, 16), but
340 add that N-acetylcarnosine and balenine were primarily enriched in human skeletal muscles, although
341 still lower than anserine and (homo)carnosine. From our systematic approach, we calculate that 99.1%
342 of the total amount of HCDs in the human body is found in skeletal muscle tissue, which confirms

343 previous estimations (28). Moreover, HCD concentrations in the present study are often different than
344 those previously reported. More specifically, we report lower HCD concentrations in human skeletal
345 muscle than previous studies (29-31). This is most likely explained by the use of tissue-specific *Carns1-*
346 *KO* tissue matrix for our quantification method, which is known to be important for MS-based
347 quantification (32). Furthermore, Peters *et al.* reported very high carnosine (1800 μ mol/kg) and
348 anserine (4000 μ mol/kg) concentrations in human kidney (23), which are approximately 1000-fold
349 higher than the concentrations in our dataset (\sim 2 μ mol/kg). Besides the use of a different detection
350 technique and quantification method, it is unclear where such differences may have originated from.

351 CARNS1 and HCDs, especially carnosine, have long been recognised as enriched compounds within the
352 olfactory tract of rodents (33, 34). Immunostaining and mass spectrometry imaging revealed the
353 enrichment of CARNS1 and carnosine in the outer (especially glomerular) layers of the mouse olfactory
354 bulb. This also highlights the potential of novel imaging techniques in future HCD research. In human
355 olfactory bulbs, we found remarkably low levels of carnosine compared to homocarnosine. In addition,
356 this is the first study to unequivocally ascribe CARNS1 expression to a specific cell type within the CNS.
357 Our discovery of CARNS1 localisation within cells of the oligodendrocyte lineage (human white matter)
358 confirms suggestions from recent RNA sequencing databases of the mouse and human CNS that
359 reported *Carns1/CARNS1* as an oligodendrocyte-enriched gene within brain parenchyma (35, 36).

360 Traditionally, the highest HCD levels are assigned to the excitable tissues. Though this holds true with
361 respect to skeletal muscle and CNS tissue, it was quite compelling that we found extremely low
362 amounts of HCDs in cardiac muscle tissue. In contrast to previous suggestions that the rat heart
363 contains \sim 10 mM HCDs (37), we report 100-fold lower levels. This was consistently found in all three
364 species we investigated, and is also 50- to 100-fold lower compared to the concentrations in skeletal
365 muscle. This can potentially be attributed to more accurate and sensitive quantification compared to
366 the older technology. Nevertheless, HCDs are thought to play a crucial role in cardiac function and
367 recovery from injury (12, 38). For instance, isolated cardiac myocytes from *Carns1*-transgenic hearts
368 were protected against hypoxia reoxygenation injury (39), whilst *Carns1*-KO rats have impaired cardiac
369 contractility accompanied by reduced Ca^{2+} peaks and slowed Ca^{2+} removal (40). This underscores the
370 physiological importance of HCDs and indicates that even low HCD levels can contribute significantly
371 to cell/organ function and health. It remains to be determined, however, which biochemical properties
372 and physiological roles of these pleiotropic molecules are the most important in different tissues and
373 under different conditions. With respect to cardiomyocytes, it has been proposed that carnosine
374 functions as a $\text{Ca}^{2+}/\text{H}^+$ exchanger to shuttle calcium towards and protons away from the sarcomere site
375 (41, 42).

376 The parent HCDs carnosine and homocarnosine share the same synthesizing enzyme CARNS1. This also
377 underlies our observation that oral β -alanine intake leads to increased carnosine but reduced
378 homocarnosine levels in human muscle, implying substrate inhibition between GABA and β -alanine for
379 CARNS1. Additionally, high expression of CARNS1 can lead to high tissue content of either carnosine
380 or homocarnosine, probably dependent of the local precursor availability (GABA vs. β -alanine). *Carns1-*
381 KO mice did not produce HCDs, whereas in WT mice, rats and humans, there appears to be a
382 relationship between CARNS1 expression and HCD content on a whole-body level. Moreover, the
383 differences in HCD content between slow- and fast-twitch muscle fibers were paralleled by similar
384 differences in CARNS1 expression. However, the correlation between CARNS1 expression and HCD
385 content was not perfect, suggesting that there might be inter-organ exchange or that there is higher
386 HCD turnover in tissues that have an important role for carnosine consumption/recycling, for example
387 through oxidative stress and reactions with toxic metabolites in pathological conditions (8).
388 Alternatively, the fact that CARNS1 shows a preference for β -alanine compared to GABA as a substrate
389 may skew this relationship considering that some tissues contain more carnosine than homocarnosine
390 and vice versa (11).

391 Tissues that have no or minimal CARNS1 expression likely rely on transmembrane uptake of HCDs
392 derived from exogenous/dietary sources or from production in CARNS1-expressing organs. It has
393 remained unclear, however, if and how HCDs are transported between tissues. The detection of HCDs
394 in various rodent and human tissues likely illustrates that HCDs can be exchanged between organs with
395 and without synthesizing capacity. Indeed, mice that lack the carnosine transporter PEPT2 have altered
396 (mostly reduced) HCD levels in various organs but increased levels in skeletal muscle tissue, which is
397 capable of synthesizing carnosine itself (22). This issue remains largely unclear in humans, in which
398 high activity of the CN1 enzyme quickly degrades circulating carnosine (2). It has long been suggested
399 that circulating HCDs are extremely low or absent in human plasma (43-45), although more recent
400 reports already detected carnosine (46, 47). We now demonstrate that N-acetylcarnosine is the most
401 stable carnosine analog in plasma, indicating that acetylation of the β -alanine residue protects against
402 the hydrolyzing activity of CN1. Thus, N-acetylcarnosine may be the primary HCD that is exchanged
403 between tissues in humans. Interestingly, plasma N-acetylcarnosine levels were correlated to muscle
404 carnosine (and N-acetylcarnosine) levels, possibly indicating that plasma N-acetylcarnosine can serve
405 as a surrogate marker for intramuscular HCD levels. Plasma N-acetylcarnosine levels increased
406 following β -alanine intake, showing that circulating N-acetylcarnosine levels may also be a marker for
407 muscle carnosine/HCD loading. In addition, our data indicate that transport of carnosine in RBCs is an
408 alternative strategy to protect against CN1 in human plasma, as recently suggested (48). This was not

409 true for rodents, who had lower HCD levels in RBCs than humans, despite more than 25 times higher
410 plasma HCD levels.

411 It has been proposed that carnosine is released from muscles during periods of contractile activity,
412 potentially serving as a health-promoting myokine. This hypothesis is primarily based on a study in
413 rats, where plasma carnosine levels increased during the dark/active phase when animals were
414 provided with a running wheel (49). We report that in humans, N-acetylcarnosine is the only HCD that
415 is consistently released from muscle tissue into plasma at rest, which is further increased during
416 periods of muscular activity (exercise). This opens various new research avenues on N-acetylcarnosine
417 as an exercise-induced myokine (50, 51). Future experiments should determine its relevance for
418 exercise training adaptations and cell/organ crosstalk (52). The average N-acetylcarnosine release of
419 14.3 nmol/min from non-contracting leg muscles at rest is striking. Extrapolation of this release to the
420 whole body, assuming that all muscles have the same N-acetylcarnosine secretion, suggests that in
421 theory the blood N-acetylcarnosine concentration should increase by 23.9 μ M every 24 hours. Despite
422 this continuous and substantial release of N-acetylcarnosine into the circulation, resting plasma N-
423 acetylcarnosine levels only reach 50-350 nM in most subjects, indicating that there is a large
424 uptake/utilization of N-acetylcarnosine in other organs, or urinary excretion. Based on the amount of
425 N-acetylcarnosine release measured in arterio-venous samples from the leg, we also estimated that a
426 daily turnover of 25% of the total muscle N-acetylcarnosine pool is needed to maintain stable muscle
427 N-acetylcarnosine levels, suggesting a rather dynamic HCD homeostasis in human muscle. Specific
428 description of these calculations and used assumptions can be found in the **Supplementary Text**. In
429 muscle interstitial fluid samples, all HCDs appear to increase during exercise. However, it is hard to
430 distinguish physiological exercise-induced release from sarcolemmal rupture caused by insertion of
431 the microdialysis probes (19), as also supported by (I) the absence of a carnosine release during
432 electrical stimulation of primary human muscle cells or interstitial fluid sampled from mice post-
433 exercise, and (II) the lack of other HCD release (besides N-acetylcarnosine) in the venous effluent of
434 contracting muscles.

435 Despite being the first study to systematically and extensively study the distribution of HCDs in three
436 species, we acknowledge that the mouse and rat data cannot be fully extrapolated to all mouse and
437 rat strains, since these can differ somewhat (53). We also decided to focus on the two parent HCDs
438 (carnosine and homocarnosine) and carnosine's methylated and acetylated analogs (anserine,
439 balenine, N-acetylcarnosine). Other HCD conjugates do exist, but these are mostly very low abundant
440 products from reactions with other (toxic) compounds (e.g. carnosine-propanol or 2-oxo-carnosine
441 (54-56)).

442 In conclusion, we extensively profiled the organ distribution of the five main HCDs and discovered new
443 physiological routes of HCD metabolism. Our results can be used to generate various new research
444 hypotheses and highlight that findings derived from animal research on HCDs can not always be
445 translated to humans. In particular, the apparent inter-cell and inter-tissue para- and endocrine
446 regulation of HCDs, as well as its relevance to human health, disease and exercise
447 performance/adaptation, deserve further investigation.

448 Materials and methods

449 HCD profiling - Rodent tissue collection

450 All mouse tissues were obtained from an in-house breeding of *Carns1-KO* and WT mice with a C57/BL6
451 background, kindly provided by Prof. M. Eckhardt (14, 57). Genotypes of the offspring from
452 heterozygous parents were determined in toe samples using a previously published protocol (14).
453 Wistar rats were supplied by Envigo (The Netherlands). Mice and rats were housed under standard
454 room conditions (12h:12h light:dark cycle, 20-24°C, relative humidity 30-60%) and had *ad libitum*
455 access to drinking water and food pellets. For tissue collection, female and male animals were
456 sacrificed at an age of 6-10 w (mice) or 7-8 w (rats) old. Following overdose injection of Dolethal
457 (200 mg/kg, i.p.), blood was collected from the right ventricle, kept in Multivette® 600 K3 EDTA vials
458 on ice, centrifuged (5 min, 3500 rpm), and plasma was stored at -80°C. Before tissue dissection, mice
459 and rats were perfused with 0.9% NaCl solution containing heparin (25 UI/mL) via a left ventricular
460 puncture. For determination of HCD levels by UHPLC-MS/MS and CARNS1 expression by Western blot,
461 tissues were immediately frozen in liquid nitrogen, before being stored at -80°C. For
462 immunohistochemistry, whole mouse brains were carefully placed on a metal plate cooled by dry ice
463 in a foam box for several minutes, wrapped in aluminum foil, and stored at -80°C. Mouse exercise
464 experiments were performed on a treadmill (6 m/min, speed increased every 2 min by 2 m/min until
465 16 m/min, total duration 60 min), and were preceded by a 1-week adaptation period (3 running
466 sessions, gradually increasing exercise intensity and duration). Sedentary mice were placed on a
467 stationary treadmill for 60 min. Immediately after exercise, plasma was obtained and mice were
468 perfused as described above. To collect interstitial fluid, gastrocnemius muscles were placed on 20 µM
469 nylon net filters (Millipore, cat# NY2004700) and centrifuged (10 min, 800 × g) (20, 21). All animal
470 procedures were approved by the Ethical Committee on Animal Experiments at Hasselt University
471 (202074B, 202127 and 202145).

472 HCD profiling - Human tissue collection

473 All human samples were obtained after written informed consent.

474 **Human vastus lateralis muscle:** Muscle biopsies were collected from the m. vastus lateralis of healthy,
475 young volunteers using the Bergström needle biopsy technique with suction, as described previously
476 (58). One part of the samples was immediately snap-frozen in liquid nitrogen and stored at -80°C until
477 UHPLC-MS/MS analysis. The other part was submerged in 1-1.5 mL of RNA/*later* (Thermo Fisher
478 Scientific), stored at 4°C for maximum 48 h and subsequently stored at -80°C for later individual fiber
479 dissection.

480 **Human heart and pectoralis muscle:** Heart and pectoralis muscle samples were collected from
481 patients undergoing open heart surgery under general anaesthesia. Heart samples consisted of the
482 right atrial appendage, harvested at the time of venous drainage cannulation for cardiopulmonary
483 bypass. Samples were immediately snap-frozen in liquid nitrogen and stored at -80°C. For **Fig 1F**, HCD
484 concentrations of vastus lateralis and pectoralis muscle were averaged.

485 **Human kidney:** Kidney samples were collected from patients undergoing radical nephrectomy. In case
486 of kidney cancer, tissue was sampled as far away from the site of the tumor to obtain the healthiest
487 part of the kidney, immediately snap-frozen in liquid nitrogen and stored at -80°C. Medulla and cortex
488 were sampled separately (**Table S1**), but data was later averaged for analysis and visualization.

489 **Human adipose tissue:** Visceral and subcutaneous adipose tissue were sampled from lean and obese
490 individuals during abdominal surgery following an overnight fast (59). Tissue pieces were rinsed, freed
491 from visible blood and connective tissue, and snap-frozen in liquid nitrogen. The two subtypes (**Table**
492 **S1**) were later averaged for analysis and visualization.

493 **Human lung:** Lung tissue was obtained from unused healthy donor lungs that were not used for
494 transplantation from the BREATH KULeuven biobank (S51577).

495 **Human liver:** Liver samples were surgically removed from fasted subjects with obesity during gastric
496 bypass surgery. Exclusion criteria were the presence of malignancies, drinking more than two units
497 (women) or three units (men) of alcohol per day, having known liver pathologies other than non-
498 alcoholic fatty liver disease. For the current analysis, five samples with NAS score 0 or 1 were selected
499 (60).

500 **Human plasma and RBC:** Blood samples were always collected in pre-cooled EDTA tubes, after a 1-2-
501 day lacto-ovo vegetarian diet to ensure no influence of dietary HCD intake. For plasma, samples were
502 immediately centrifuged (10 min, 3000 × g, 4°C), followed by immediate deproteinization (110 µL of
503 35% 5-sulfosalicylic acid per 1 mL of plasma) and second centrifugation (5 min, 15000 × g, 4°C). Plasma
504 samples were then stored at -80°C. For RBC isolation (61), blood tubes were centrifuged for 15 min at
505 120 × g at room temperature. Plasma was carefully removed and 200 µL RBCs were collected in 1.8 mL
506 of ice-cold methanol (55% v/v). Samples were then stored at -80°C.

507 **Human CNS:** Seven different human CNS regions were obtained from The Netherlands Brain Bank
508 (NBB), Netherlands Institute for Neuroscience, Amsterdam (open access www.brainbank.nl). All
509 donors were 'non-demented controls', indicating the absence of neurological and psychiatric disease.
510 From 2 subjects, all 7 regions were available. For immunohistochemical analyses, white matter tissue

511 from healthy controls and unaffected white matter tissue of multiple sclerosis patients from a previous
512 study was used.

513 **Human cerebrospinal fluid:** Cerebrospinal fluid from subjects without neurological disease at the time
514 of sampling was obtained via the University Biobank Limburg (UbiLim), with approval from the Medical
515 Ethics Committee at Hasselt University (CME2021-004). Lumbar cerebrospinal fluid was collected into
516 PPS tubes, kept at 4°C, centrifuged to remove cells (10 min, 500 × g, 4°C), and supernatant was stored
517 at -80°C.

518

519 Human β-alanine supplementation study

520 Vastus lateralis muscle biopsies obtained via the Bergström needle biopsy technique with suction
521 (n=11 β-alanine, n=11 placebo) and plasma samples (n=19 β-alanine, n=17 placebo) were collected
522 before and after 12 weeks of β-alanine supplementation in patients with COPD (sustained-release
523 CarnoSyn®, NAI). Methodological details have been described previously (62). Snap-frozen biopsies
524 were freeze-dried for 48 h, followed by manual removal of non-muscle material (fat, connective tissue,
525 blood) under a light microscope. Effects of β-alanine were analyzed using a two-way repeated
526 measures ANOVA (group vs. time) for each HCD separately, followed by Sidak's multiple comparisons
527 tests. Correlations were performed using Pearson correlation (Δ muscle carnosine vs. Δ N-
528 acetylcarnosine) or Spearman rank correlation (muscle carnosine vs. plasma N-acetylcarnosine).

529

530 Human HCD release experiments

531 **Microdialysis experiment:** Detailed methodology has been described previously (63). In short,
532 interstitial samples from m. vastus lateralis were collected using the microdialysis technique at rest
533 and after 30 min of one-legged knee extensor exercise (15 min 6 W, 15 min 50% peak power). Subjects
534 consisted of a group of young (n=7) and old (n=13) healthy men (results are pooled together since no
535 differences between groups could be observed). Concentrations were corrected for probe recovery as
536 determined by relative loss of [2-3H]-labeled adenosine in the dialysate. Interstitial levels during
537 exercise were compared to resting values using a multiple Wilcoxon matched-pairs signed rank test
538 with Holm-Sidak multiple comparison test.

539 **Arterio-venous balance experiment 1:** Arterial and venous samples were collected from the femoral
540 artery/vein at rest and after 30min one-legged knee extensor exercise (6W) in a group of healthy
541 postmenopausal women (n=19). Methodological details can be found in (64). Samples were

542 deproteinized with 35% 5-sulfosalicylic acid, as described above, on the day of the UHPLC-MS/MS
543 analysis. Exercise *vs.* resting HCD levels were compared using a multiple Wilcoxon matched-pairs
544 signed rank test with Holm-Sidak multiple comparison test.

545 **Arterio-venous balance experiment 2:** Seven healthy, young men (28 ± 4 years old, BMI of 24 ± 2 ,
546 $\text{VO}_{2\text{max}}$ of 49 ± 7 mL/min/kg) participated in this experiment. After passive transport to the lab,
547 catheters were inserted in the femoral artery and vein. Next, arterial and venous samples were
548 collected every 30 min during a 90 min supine resting period. After this, 20 min of passive leg
549 movement was performed, followed by 60 min of active one-legged knee extensor exercise (20 min 10
550 W, 20 min 20 W, 20 min 10 W). Samples were collected at the end of each exercise bout. Finally,
551 arterio-venous samples were collected after 30 min and 2 h of recovery. Plasma and RBC samples were
552 collected as described above. Exercise-induced effects were analyzed using a mixed-effect model with
553 repeated measurements over time, with post-hoc comparison of every time point *vs.* baseline (Holm-
554 Sidak test).

555

556 Primary cell culture experiments

557 Biopsy samples (~150 mg) were obtained from *m. vastus lateralis* from young, healthy men. Primary
558 skeletal muscle cells were isolated with homemade antibody-coated magnetic beads and cultured as
559 previously described (65, 66). Cultured skeletal muscle cells were used for analysis on day 5 or 6 after
560 the onset of differentiation. At this time, most of the myocytes have differentiated into multinucleated
561 myotubes and can easily be identified as muscle cells. Myotubes were starved with media containing
562 0.1% Bovine Serum Albumin (DMEM without phenol, D-glucose and L-glutamine) for 16 hours before
563 experiments. The skeletal muscle cells were electro-stimulated as described previously (67), with the
564 minor addition of 5 μ M (S)-nitro-Blebbistatin (Cayman Chemical, CAS. 856925-75-2) to the stimulation
565 buffer to inhibit the spontaneous contraction of the myotubes (68). The cells were stimulated for 2-3
566 h (50 Hz, 0.6s/0.4 s trains, 1 ms pulse width, 10 V, homemade electrical stimulator connected to a
567 Digitimer MultiStim SYSTEM-D330). The extracellular medium was collected immediately or 30 min
568 after the end of stimulation, and medium from non-stimulated control cells was harvested
569 simultaneously. Changes over time were analyzed using a mixed-effect model with repeated
570 measurements over time, with post-hoc comparison of stimulated and stimulated+recovery *vs.* control
571 cells (Holm-Sidak test).

572

573

574 HCD determination by UHPLC-MS/MS

575 Details of the validation of the in-house developed UHPLC-MS/MS analysis has been described
576 previously (69), with the exception that all experiments were performed on a Xevo® TQ-S MS/MS
577 system with 2.5 μ L injection volume. The limit of detection was determined to be 5-10 nM (in plasma),
578 corresponding to 0.38-0.76 μ mol/kg tissue for our homogenization protocol. Pure carnosine and
579 anserine were kindly provided by Flamma S.p.a. (Chignolo d'Isola, Bergamo, Italy), and pure balenine
580 by NNB Nutrition (Frisco, Texas, USA). Homocarnosine (#33695) and N-acetyl-L-carnosine (#18817)
581 were bought from Cayman Chemical (Ann Arbor, Michigan, USA). UHPLC-MS/MS data extraction and
582 analysis was performed using Masslynx software 4.2 (Waters, Milford, USA).

583 **Tissues:** All tissues were prepared similarly, based on the method described previously (8). Frozen
584 tissues were quickly weighed and immediately homogenized in extraction solution (ultrapure water
585 with 10 mM HCl and internal standard carnosine-d4) in a ratio of 95 μ L extraction solution per 5 mg
586 tissue in a QIAGEN TissueLyser II (1 min, 30 Hz). The concentration of carnosine-d4 varied according to
587 expected HCD concentrations in the tissues: muscle (20 μ M), CNS (5 μ M), liver/lung/spleen (0.5 μ M)
588 and all other tissues (1 μ M). Then, homogenates were centrifuged (20 min, 3000 \times g, 4°C).
589 Supernatants were immediately diluted in a 3:1 ratio with ice-cold acetonitrile (-20°C), vortexed and
590 kept on ice for 15min. After a second centrifugation step (20 min, 3000 \times g, 4°C), samples were stored
591 at -80°C until the day of the UHPLC-MS/MS analysis. Samples were combined with 75:25
592 acetonitrile:water in a 4:1 ratio before injection in the UHPLC-MS/MS device. For skeletal muscle and
593 CNS, samples were also injected after an extra initial dilution (1:25 for muscle, 1:10 for CNS) for the
594 determination of carnosine (skeletal muscle) and homocarnosine (CNS) content. Standard calibration
595 curves were prepared for each individual run and for each tissue separately in the respective tissue of
596 the *Carns1-KO* mice to account for possible tissue matrix effects (for all three species). Differences
597 between soleus and EDL HCD levels in mice and rats were analyzed using paired t-tests or Wilcoxon
598 signed-rank tests, depending on normality of the data.

599 **Plasma:** Deproteinized plasma (150 μ L) was combined with acetonitrile containing 1% formic acid (215
600 μ L), 1 μ M carnosine-d4 as internal standard (10 μ L) and ultrapure water (25 μ L). For mouse plasma
601 analysis, volumes were scaled down to available plasma (75 μ L). After thoroughly vortexing, samples
602 were centrifuged (15 min, 15000 \times g, 4°C). The supernatant was collected and injected in the UHPLC-
603 MS/MS. A standard calibration curve was prepared in a pool of human deproteinized plasma that was
604 collected after a 2-day lacto-ovo vegetarian diet to minimize circulating HCDs (for all three species).

605 **RBC:** First, 190 μ L of the RBC samples was combined with 10 μ L of internal standard carnosine-d4
606 (2 μ M) and 10 μ L of 75:25 acetonitrile:water (with 1% formic acid). This mixture was vortexed and then

607 centrifuged in a 10 kDa filter (Nanosep® Centrifugal Device with Omega Membrane™, Pall
608 Corporation). The supernatant was subsequently evaporated at 40°C and the droplet resuspended in
609 40 µL of 75:25 acetonitrile:water (with 1% formic acid) before injection in the UHPLC-MS/MS device.
610 A standard calibration curve was prepared in a pool of human RBC samples that were collected after a
611 2-day lacto-ovo vegetarian diet to minimize circulating HCDs (for all three species).

612 **Cerebrospinal fluid:** Human cerebrospinal fluid was treated identically as plasma, but the standard
613 calibration curve was prepared in ultrapure water since no *Carns1*-KO tissue matrix was available,
614 possibly resulting in overestimation of the absolute concentrations.

615 **Interstitial fluid:** Interstitial fluid (15 µL) was combined with 30 µL acetonitrile containing 1% formic
616 acid and 1 µM carnosine-d4 and 10 µL ultrapure water. This mixture was vortexed, centrifuged (15
617 min, 15000 × g, 4°C) and the supernatant was used to inject in the UHPLC-MS/MS. For detection of
618 carnosine in humans, samples were first diluted 1:30. For detection of carnosine and anserine in mice,
619 samples were first diluted 1:500. A standard calibration curve was prepared in Ringer-Acetate buffer
620 as this was used to perfuse the microdialysis probes.

621 **Cell culture medium:** Extracellular medium (150 µL) was mixed with acetonitrile containing 1% formic
622 acid (240 µL) and internal standard carnosine-d4 (2 µM, 10 µL), vortexed and injected in the UHPLC-
623 MS/MS. A standard calibration curve was prepared in DMEM culture medium.

624

625 CARNS1 protein levels by Western blot

626 Tissues were diluted in RIPA buffer (300 µL per 10 mg tissue; 50 mM Tris pH 8.0, 150 mM NaCl, 0.5%
627 sodium deoxycholate, 0.1% SDS, 1% Triton-X100, and freshly added protease/phosphatase inhibitors
628 [Roche]), and homogenized using stainless steel beads and a QIAGEN TissueLyser II (shaking 1 min, 30
629 Hz). Following centrifugation (15 min, 12000 × g, 4°C), supernatants were stored at -80°C. Pierce™ BCA
630 Protein Assay Kit (Thermo Fisher) was used according to manufacturer's instructions to determine
631 protein concentrations (read at 570 nm wavelength). For detection of CARNS1 protein levels, 1 µg of
632 protein was diluted in loading buffer solution (63 mM Tris Base pH 6.8, 2% SDS, 10% glycerol, 0.004%
633 Bromophenol Blue, 0.1 M DTT), heated for 4 min at 95°C, and separated in polyacrylamide gels (4-15%,
634 Mini-PROTEAN TGX, Bio-Rad) at 100-140 V on ice. Next, stain-free gels were imaged following UV
635 exposure to visualise total protein content (ChemiDoc MP Imaging System, Bio-Rad). Proteins were
636 transferred from the gel to an ethanol-immersed PVDF membrane in transfer buffer (30 min, 25 V, 1.0
637 A, Trans-Blot Turbo Transfer System, Bio-Rad). Membranes were briefly washed in Tris-buffered saline
638 with 0.1% Tween20 (TBS-T), and blocked for 30 min using 3% milk powder in TBS-T. Following overnight

639 incubation at 4°C with primary antibodies against CARNS1 (rabbit polyclonal, 1:1000 in 3% milk/TBS-T,
640 HPA038569, Sigma), membranes were washed (3 × 5 min), incubated with secondary HRP-conjugated
641 goat anti-rabbit antibodies (1:5000 in 3% milk/TBS-T) for 60 min at room temperature, washed again
642 (3 × 5 min), and chemiluminescent images were developed in a ChemiDoc MP Imaging System (Bio-
643 Rad) using Clarity Western ECL substrate (Bio-Rad). CARNS1 protein bands were quantified with Image
644 Lab 6.1 software (Bio-Rad), and normalized to total protein content from the stain-free image. Finally,
645 bands were expressed relative to total CARNS1 expression (sum of all bands) of a particular mouse,
646 rat, or human. For muscle, band densities were expressed as fold changes relative to the average
647 density from soleus muscles per blot. Linearity of the signal was determined for every tissue.
648 Differences between soleus and extensor digitorum longus CARNS1 content were analyzed using a
649 paired t-test (rat) or Wilcoxon signed-rank test (mouse), depending on normality of the data.

650

651 CARNS1 protein level in human single muscle fibers.

652 CARNS1 protein levels in type I vs. type II muscle fibers were determined based on a previously
653 published method (70). Muscle samples in RNAlater (Thermo Fisher Scientific) were thawed and
654 subsequently transferred to a petri dish filled with fresh RNAlater (Thermo Fisher Scientific) solution.
655 Individual muscle fibers were manually dissected under a light microscope and immediately
656 submerged in a new 0.5 mL tube with 5 µL ice-cold Laemmli buffer (125 mM Tris-HCl (pH 6.8), 10%
657 glycerol, 125 mM SDS, 200 mM DTT, 0.004% bromophenol blue). Tubes were then incubated for 15
658 min at 4°C, followed by 10 min at 70°C and then stored at -80°C until the next step of the analysis. A
659 total of 40-72 fibers were isolated from 9 biopsies. Next, muscle fiber type (based on myosin heavy
660 chain expression) was determined using dot blotting techniques. For this, 0.5 µL of the muscle fiber
661 lysate was spotted onto two activated and equilibrated PVDF membranes, one for MHC I and one for
662 MHC IIa. After air-drying the PVDF membrane for 30 min, it was re-activated in 96% ethanol and
663 equilibrated in transfer buffer (8 mM Tris-base, 39 mM glycine, 0.015% SDS, 20% ethanol). The next
664 steps are similar to standard Western blotting as described above, with primary antibodies for MHC I
665 (A4.840, 1:1000 in 3% milk in TBS-T, DSHB) or MHC IIa (A4.74, 1:1000 in 3% milk in TBS-T, DSHB). Fiber
666 lysates were classified as type I or IIa fibers based on a positive stain for only the MHC I or IIa antibody
667 (**Fig S1**). Next, fibers of the same type from the same subject were pooled (n=10-26 for type I and n=9-
668 22 for type IIa fibers). CARNS1 protein content in these fiber type-specific samples were determined
669 with standard Western blotting technique as described above, with loading of 5 µL per pool. Band
670 densities were expressed as fold changes relative to the average density from type I fibers per blot.
671 Statistical analysis was performed using a Wilcoxon signed-rank test.

672 *CARNS1* mRNA expression

673 The fiber type-specific RNAseq dataset of Rubenstein *et al.* was downloaded from the GEO repository
674 under accession number GSE130977 (18). This dataset consists of RNAseq data of pools of type I or
675 type II fibers from *m. vastus lateralis* biopsies of 9 healthy, older men. For full details on generation of
676 this dataset, we refer to the original publication. Raw counts were normalized with DESeq2 to allow
677 for between-sample comparisons (71). First, normalized counts for *MYH2* (ENSG00000125414, type II
678 fibers) and *MYH7* (ENSG00000092054, type I fibers) were extracted and assessed for each fiber pool
679 as purity quality control. Based on this analysis, the fiber pools of one participant were excluded for
680 further analysis. Next, normalized counts of *CARNS1* (ENSG00000172508) were extracted and
681 compared between type I and type II fiber pools within each participant using a Wilcoxon signed-rank
682 test.

683

684 Immunohistochemical detection of *CARNS1*

685 Sagittal and frontal cryosections (10 μm) were cut from whole mouse brains and human white matter
686 samples. Following acetone fixation (10 min) and blocking (30 min, 10% donkey serum in PBS with 1%
687 BSA), sections were exposed overnight at 4°C to antibodies detecting *CARNS1* (rabbit polyclonal, 1:100
688 in PBS with 1% BSA, HPA038569, Sigma). The next day, sections were washed and exposed to
689 complementary secondary antibodies for 60 min (1:500 in PBS with 1% BSA, Thermo Fisher).
690 Fluorescence imaging was performed with a Leica DM4000 B LED (Leica Microsystems). For double-
691 labeling, we used the following antibodies: *OLIG2* (1:50, goat polyclonal, AF2418, R&D Systems),
692 neurofilament heavy polypeptide (NF-H, rabbit polyclonal, 1:200, ab8135, Abcam), *CD68* (mouse
693 monoclonal, 1:100, M0814 KP1 clone, Dako), *GFAP* (mouse monoclonal, 1:100, G3893, Sigma).
694 Absence of *CARNS1* from *Carns1*-KO brain sections was used as negative control.

695

696 Matrix-assisted laser desorption ionization mass spectrometry imaging (MALDI-MSI)

697 The spatial distribution of carnosine and homocarnosine was studied in mouse brains by MALDI-MSI.
698 Fresh DHB solution (20 mg/mL in 70% MeOH with 0.2% Trifluoroacetic acid) was sprayed using TM-
699 sprayer (HTX Technologies) in a series of 15 layers with the settings: temperature 75°C, pressure 10
700 psi, flow rate 0.12 mL/min, velocity 1200 mm/min, track spacing 2 mm. MS acquisition was conducted
701 on a Tims-TOF mass spectrometer (Bruker Daltonik GmbH). The data were acquired at a raster size of
702 50 \times 50 μm (or 20 \times 20 μm for higher spatial resolution) in the mass range of 100-800 *m/z* in positive
703 ion mode (300 laser shots per pixel with 5000 Hz frequency). After performing the MALDI-MSI
704 experiments, the matrix was gently removed by submersion in EtOH for 2 min. Slides were then

705 washed in serial baths containing 100% EtOH, 90% EtOH, 70% EtOH or ultrapure water for 3 min each.
706 The sections were stained by hematoxylin for 3 min, and eosin for 20 seconds. Following dehydrating
707 steps, digital images were acquired with the Mirax system (Carl Zeiss) at 40 \times magnification and
708 uploaded on Aperio ImageScope (Leica Biosystems).

709

710 Statistical analysis

711 Statistical analyses were performed in GraphPad Prism v9.4 and were described in the appropriate
712 method paragraphs. Significance level was set at $\alpha=0.05$.

713

714 **References**

- 715 1. W. Gulewitsch, S. Amiradžibi, Ueber das Carnosin, eine neue organische Base des
716 Fleischextractes. *Berichte der deutschen chemischen Gesellschaft* **33**, 1902-1903 (1900).
- 717 2. A. A. Boldyrev, G. Aldini, W. Derave, Physiology and pathophysiology of carnosine. *Physiological reviews* **93**, 1803-1845 (2013).
- 718 3. G. Aldini, B. de Courten, L. Regazzoni, E. Gilardoni, G. Ferrario, G. Baron, A. Altomare, A.
719 D'Amato, G. Vistoli, M. Carini, Understanding the antioxidant and carbonyl sequestering
720 activity of carnosine: Direct and indirect mechanisms. *Free Radical Research* **55**, 321-330
721 (2021).
- 722 4. J. J. Matthews, M. D. Turner, L. Santos, K. J. Elliott-Sale, C. Sale, Carnosine increases insulin-
723 stimulated glucose uptake and reduces methylglyoxal-modified proteins in type-2 diabetic
724 human skeletal muscle cells. *Amino Acids*, 1-8 (2023).
- 725 5. B. Saunders, K. Elliott-Sale, G. G. Artioli, P. A. Swinton, E. Dolan, H. Roschel, C. Sale, B. Gualano,
726 β -alanine supplementation to improve exercise capacity and performance: a systematic
727 review and meta-analysis. *British Journal of Sports Medicine* **51**, 658-669 (2017).
- 728 6. G. Aldini, M. Orioli, G. Rossoni, F. Savi, P. Braidotti, G. Vistoli, K. J. Yeum, G. Negrisoli, M. Carini,
729 The carbonyl scavenger carnosine ameliorates dyslipidaemia and renal function in Zucker
730 obese rats. *Journal of cellular and molecular medicine* **15**, 1339-1354 (2011).
- 731 7. E. J. Anderson, G. Vistoli, L. A. Katunga, K. Funai, L. Regazzoni, T. B. Monroe, E. Gilardoni, L.
732 Cannizzaro, M. Colzani, D. De Maddis, A carnosine analog mitigates metabolic disorders of
733 obesity by reducing carbonyl stress. *The Journal of clinical investigation* **128**, 5280-5293 (2018).
- 734 8. J. Spaas, W. Franssen, C. Keytsman, L. Blancquaert, T. Vanmierlo, J. Bogie, B. Broux, N. Hellings,
735 J. van Horssen, D. K. Posa, Carnosine quenches the reactive carbonyl acrolein in the central
736 nervous system and attenuates autoimmune neuroinflammation. *Journal of
737 neuroinflammation* **18**, 1-19 (2021).
- 738 9. I. Everaert, Y. Taes, E. De Heer, H. Baelde, A. Zutinic, B. Yard, S. Sauerhöfer, L. Vanhee, J.
739 Delanghe, G. Aldini, Low plasma carnosinase activity promotes carnosinemia after carnosine
740 ingestion in humans. *American Journal of Physiology-Renal Physiology*, (2012).
- 741 10. M. Teufel, V. Saudek, J.-P. Ledig, A. Bernhardt, S. Boulard, A. Carreau, N. J. Cairns, C. Carter,
742 D. J. Cowley, D. Duverger, Sequence identification and characterization of human carnosinase
743 and a closely related non-specific dipeptidase. *Journal of Biological Chemistry* **278**, 6521-6531
744 (2003).
- 745

746 11. J. Drozak, M. Veiga-da-Cunha, D. Vertommen, V. Stroobant, E. Van Schaftingen, Molecular
747 identification of carnosine synthase as ATP-grasp domain-containing protein 1 (ATPGD1).
748 *Journal of biological chemistry* **285**, 9346-9356 (2010).

749 12. J. V. Creighton, L. de Souza Gonçalves, G. G. Artioli, D. Tan, K. J. Elliott-Sale, M. D. Turner, C. L.
750 Doig, C. Sale, Physiological Roles of Carnosine in Myocardial Function and Health. *Advances in
751 Nutrition* **13**, 1914-1929 (2022).

752 13. G. Aldini, M. Orioli, M. Carini, R. Maffei Facino, Profiling histidine-containing dipeptides in rat
753 tissues by liquid chromatography/electrospray ionization tandem mass spectrometry. *Journal of mass
754 spectrometry* **39**, 1417-1428 (2004).

755 14. L. Wang-Eckhardt, A. Bastian, T. Bruegmann, P. Sasse, M. Eckhardt, Carnosine synthase
756 deficiency is compatible with normal skeletal muscle and olfactory function but causes
757 reduced olfactory sensitivity in aging mice. *Journal of Biological Chemistry*, jbc. RA120. 014188
758 (2020).

759 15. J. Spaas, P. Van Noten, C. Keytsman, I. Nieste, L. Blancquaert, W. Derave, B. O. Eijnde,
760 Carnosine and skeletal muscle dysfunction in a rodent multiple sclerosis model. *Amino Acids*
761 **53**, 1749-1761 (2021).

762 16. I. Everaert, S. Stegen, B. Vanheel, Y. Taes, W. Derave, Effect of beta-alanine and carnosine
763 supplementation on muscle contractility in mice. *Med Sci Sports Exerc* **45**, 43-51 (2013).

764 17. L. Luo, W. Ma, K. Liang, Y. Wang, J. Su, R. Liu, T. Liu, N. Shyh-Chang, Spatial metabolomics
765 reveals skeletal myofiber subtypes. *Science Advances* **9**, eadd0455 (2023).

766 18. A. B. Rubenstein, G. R. Smith, U. Raue, G. Begue, K. Minchev, F. Ruf-Zamojski, V. D. Nair, X.
767 Wang, L. Zhou, E. Zaslavsky, Single-cell transcriptional profiles in human skeletal muscle.
768 *Scientific reports* **10**, 1-15 (2020).

769 19. N. Nordsborg, M. Mohr, L. D. Pedersen, J. J. Nielsen, H. Langberg, J. Bangsbo, Muscle interstitial
770 potassium kinetics during intense exhaustive exercise: effect of previous arm exercise.
771 *American Journal of Physiology-Regulatory, Integrative and Comparative Physiology* **285**,
772 R143-R148 (2003).

773 20. A. Reddy, L. H. Bozi, O. K. Yaghi, E. L. Mills, H. Xiao, H. E. Nicholson, M. Paschini, J. A. Paulo, R.
774 Garrity, D. Laznik-Bogoslavski, pH-gated succinate secretion regulates muscle remodeling in
775 response to exercise. *Cell* **183**, 62-75. e17 (2020).

776 21. M. J. Mittenbühler, M. P. Jedrychowski, J. G. Van Vranken, H.-G. Sprenger, S. Wilensky, P. A.
777 Dumesic, Y. Sun, A. Tartaglia, D. Bogoslavski, A. Mu, Isolation of extracellular fluids reveals
778 novel secreted bioactive proteins from muscle and fat tissues. *Cell Metabolism*, (2023).

779 22. M. A. Kamal, H. Jiang, Y. Hu, R. F. Keep, D. E. Smith, Influence of genetic knockout of Pept2 on
780 the in vivo disposition of endogenous and exogenous carnosine in wild-type and Pept2 null
781 mice. *American Journal of Physiology-Regulatory, Integrative and Comparative Physiology* **296**,
782 R986-R991 (2009).

783 23. V. Peters, C. Q. Klessens, H. J. Baelde, B. Singler, K. A. Veraar, A. Zutinic, J. Drozak, J. Zschocke,
784 C. P. Schmitt, E. de Heer, Intrinsic carnosine metabolism in the human kidney. *Amino acids* **47**,
785 2541-2550 (2015).

786 24. T. Weigand, F. Colbatzky, T. Pfeffer, S. F. Garbade, K. Klingbeil, F. Colbatzky, M. Becker, J.
787 Zemva, R. Bulkescher, R. Schürfeld, A global Cndp1-knock-out selectively increases renal
788 carnosine and anserine concentrations in an age-and gender-specific manner in mice.
789 *International journal of molecular sciences* **21**, 4887 (2020).

790 25. E. Heidenreich, T. Pfeffer, T. Kracke, N. Mechtel, P. Nawroth, G. F. Hoffmann, C. P. Schmitt, R.
791 Hell, G. Poschet, V. Peters, A Novel UPLC-MS/MS Method Identifies Organ-Specific Dipeptide
792 Profiles. *International journal of molecular sciences* **22**, 9979 (2021).

793 26. D. Abraham, J. J. Pisano, S. Udenfriend, The distribution of homocarnosine in mammals.
794 *Archives of biochemistry and biophysics* **99**, 210-213 (1962).

795 27. S. J. Kish, T. L. Perry, S. Hansen, Regional distribution of homocarnosine, homocarnosine-
796 carnosine synthetase and homocarnosinase in human brain. *Journal of neurochemistry* **32**,
797 1629-1636 (1979).

798 28. W. Derave, I. Everaert, S. Beeckman, A. Baguet, Muscle carnosine metabolism and β -alanine
799 supplementation in relation to exercise and training. *Sports medicine* **40**, 247-263 (2010).

800 29. A. Mannion, P. Jakeman, M. Dunnett, R. Harris, P. Willan, Carnosine and anserine
801 concentrations in the quadriceps femoris muscle of healthy humans. *European journal of*
802 *applied physiology and occupational physiology* **64**, 47-50 (1992).

803 30. R. C. Harris, M. Dunnett, P. L. Greenhaff, Carnosine and taurine contents in individual fibres of
804 human vastus lateralis muscle. *Journal of Sports Sciences* **16**, 639-643 (1998).

805 31. A. Baguet, I. Everaert, H. De Naeyer, H. Reyngoudt, S. Stegen, S. Beeckman, E. Achten, L.
806 Vanhee, A. Volkaert, M. Petrovic, Effects of sprint training combined with vegetarian or mixed
807 diet on muscle carnosine content and buffering capacity. *European journal of applied*
808 *physiology* **111**, 2571-2580 (2011).

809 32. W. Zhou, S. Yang, P. G. Wang. (Future Science, 2017), vol. 9, pp. 1839-1844.

810 33. F. L. Margolis, Carnosine in the primary olfactory pathway. *Science* **184**, 909-911 (1974).

811 34. E. Mahootchi, S. Cannon Homaei, R. Kleppe, I. Winge, T.-A. Hegvik, R. Megias-Perez, C. Totland,
812 F. Mogavero, A. Baumann, J. C. Glennon, GADL1 is a multifunctional decarboxylase with tissue-
813 specific roles in β -alanine and carnosine production. *Science Advances* **6**, eabb3713 (2020).

814 35. Y. Zhang, K. Chen, S. A. Sloan, M. L. Bennett, A. R. Scholze, S. O'Keeffe, H. P. Phatnani, P.
815 Guarnieri, C. Caneda, N. Ruderisch, An RNA-sequencing transcriptome and splicing database
816 of glia, neurons, and vascular cells of the cerebral cortex. *Journal of Neuroscience* **34**, 11929-
817 11947 (2014).

818 36. T. M. Consortium, S. t. w. group, Single-cell transcriptomics of 20 mouse organs creates a
819 Tabula Muris. *Nature* **562**, 367-372 (2018).

820 37. J. J. O'Dowd, D. J. Robins, D. J. Miller, Detection, characterisation, and quantification of
821 carnosine and other histidyl derivatives in cardiac and skeletal muscle. *Biochimica et*
822 *Biophysica Acta (BBA)-General Subjects* **967**, 241-249 (1988).

823 38. K. Yan, Z. Mei, J. Zhao, M. A. I. Prodhan, D. Obal, K. Katragadda, B. Doelling, D. Hoetker, D. K.
824 Posa, L. He, Integrated Multilayer Omics Reveals the Genomic, Proteomic, and Metabolic
825 Influences of Histidyl Dipeptides on the Heart. *Journal of the American Heart Association* **11**,
826 e023868 (2022).

827 39. J. Zhao, D. J. Conklin, Y. Guo, X. Zhang, D. Obal, L. Guo, G. Jagatheesan, K. Katragadda, L. He, X.
828 Yin, Cardiospecific Overexpression of ATPGD1 (Carnosine Synthase) Increases Histidine
829 Dipeptide Levels and Prevents Myocardial Ischemia Reperfusion Injury. *Journal of the*
830 *American Heart Association*, e015222 (2020).

831 40. L. de Souza Gonçalves, L. P. Sales, T. R. Saito, J. C. Campos, A. L. Fernandes, J. Natali, L. Jensen,
832 A. Arnold, L. Ramalho, L. R. G. Bechara, Histidine dipeptides are key regulators of excitation-
833 contraction coupling in cardiac muscle: Evidence from a novel CARNS1 knockout rat model.
834 *Redox biology* **44**, 102016 (2021).

835 41. P. Swietach, J.-B. Youm, N. Saegusa, C.-H. Leem, K. W. Spitzer, R. D. Vaughan-Jones, Coupled
836 Ca²⁺/H⁺ transport by cytoplasmic buffers regulates local Ca²⁺ and H⁺ ion signaling.
837 *Proceedings of the National Academy of Sciences* **110**, E2064-E2073 (2013).

838 42. P. Swietach, C. H. Leem, K. W. Spitzer, R. D. Vaughan-Jones, Pumping Ca²⁺ up H⁺ gradients: A
839 Ca²⁺-H⁺ exchanger without a membrane. *The Journal of physiology* **592**, 3179-3188 (2014).

840 43. M. Gardner, K. M. Illingworth, J. Kelleher, D. Wood, Intestinal absorption of the intact peptide
841 carnosine in man, and comparison with intestinal permeability to lactulose. *The Journal of*
842 *physiology* **439**, 411-422 (1991).

843 44. R. C. Harris, M. Tallon, M. Dunnett, L. Boobis, J. Coakley, H. J. Kim, J. L. Fallowfield, C. Hill, C.
844 Sale, J. A. Wise, The absorption of orally supplied β -alanine and its effect on muscle carnosine
845 synthesis in human vastus lateralis. *Amino acids* **30**, 279-289 (2006).

846 45. A. Baguet, I. Everaert, B. Yard, V. Peters, J. Zschocke, A. Zutinic, E. De Heer, T. Podgórski, K.
847 Domaszewska, W. Derave, Does low serum carnosinase activity favour high-intensity exercise
848 capacity? *American Journal of Physiology-Heart and Circulatory Physiology*, (2014).

849 46. V. K. Pandya, B. Sonwane, R. Rathore, A. Unnikrishnan, S. Kumaran, M. J. Kulkarni,
850 Development of multiple reaction monitoring assay for quantification of carnosine in human
851 plasma. *RSC advances* **10**, 763-769 (2020).

852 47. S. de Jager, L. Blancquaert, T. Van der Stede, E. Lievens, S. De Baere, S. Croubels, E. Gilardoni,
853 L. G. Regazzoni, G. Aldini, J. G. Bourgois, The ergogenic effect of acute carnosine and anserine
854 supplementation: dosing, timing, and underlying mechanism. *Journal of the International
855 Society of Sports Nutrition* **19**, 70-91 (2022).

856 48. H. Oppermann, S. Elsel, C. Birkemeyer, J. Meixensberger, F. Gaunitz, Erythrocytes prevent
857 degradation of carnosine by human serum carnosinase. *International journal of molecular
858 sciences* **22**, 12802 (2021).

859 49. K. Nagai, A. Niijima, T. Yamano, H. Otani, N. Okumura, N. Tsuruoka, M. Nakai, Y. Kiso, Possible
860 role of L-carnosine in the regulation of blood glucose through controlling autonomic nerves.
861 *Experimental biology and medicine* **228**, 1138-1145 (2003).

862 50. M. C. K. Severinsen, B. K. Pedersen, Muscle–organ crosstalk: the emerging roles of myokines.
863 *Endocrine reviews* **41**, 594-609 (2020).

864 51. B. K. Pedersen, M. A. Febbraio, Muscles, exercise and obesity: skeletal muscle as a secretory
865 organ. *Nature Reviews Endocrinology* **8**, 457-465 (2012).

866 52. R. M. Murphy, M. J. Watt, M. A. Febbraio, Metabolic communication during exercise. *Nature
867 metabolism* **2**, 805-816 (2020).

868 53. M. E. Nelson, S. Madsen, K. C. Cooke, A. M. Fritzen, I. H. Thorius, S. W. Masson, L. Carroll, F. C.
869 Weiss, M. M. Seldin, M. Potter, Systems-level analysis of insulin action in mouse strains
870 provides insight into tissue-and pathway-specific interactions that drive insulin resistance. *Cell
871 Metabolism* **34**, 227-239. e226 (2022).

872 54. H. Ihara, Y. Kakihana, A. Yamakage, K. Kai, T. Shibata, M. Nishida, K.-i. Yamada, K. Uchida, 2-
873 Oxo-histidine-containing dipeptides are functional oxidation products. *Journal of Biological
874 Chemistry* **294**, 1279-1289 (2019).

875 55. S. P. Baba, J. D. Hoetker, M. Merchant, J. B. Klein, J. Cai, O. A. Barski, D. J. Conklin, A. Bhatnagar,
876 Role of aldose reductase in the metabolism and detoxification of carnosine-acrolein
877 conjugates. *Journal of Biological Chemistry* **288**, 28163-28179 (2013).

878 56. V. H. Carvalho, A. H. Oliveira, L. F. de Oliveira, R. P. da Silva, P. Di Mascio, B. Gualano, G. G.
879 Artioli, M. H. Medeiros, Exercise and β -alanine supplementation on carnosine-acrolein adduct
880 in skeletal muscle. *Redox biology* **18**, 222-228 (2018).

881 57. L. Wang-Eckhardt, I. Becker, Y. Wang, J. Yuan, M. Eckhardt, Absence of endogenous carnosine
882 synthesis does not increase protein carbonylation and advanced lipoxidation end products in
883 brain, kidney or muscle. *Amino Acids*, 1-11 (2022).

884 58. T. Van der Stede, L. Blancquaert, F. Stassen, I. Everaert, R. Van Thienen, C. Vervaet, L.
885 Gliemann, Y. Hellsten, W. Derave, Histamine H1 and H2 receptors are essential transducers of
886 the integrative exercise training response in humans. *Science Advances* **7**, eabf2856 (2021).

887 59. K. Verboven, K. Wouters, K. Gaens, D. Hansen, M. Bijnen, S. Wetzels, C. D. Stehouwer, G. H.
888 Goossens, C. G. Schalkwijk, E. E. Blaak, Abdominal subcutaneous and visceral adipocyte size,
889 lipolysis and inflammation relate to insulin resistance in male obese humans. *Scientific reports*
890 **8**, 1-8 (2018).

891 60. F. Van de Velde, D. M. Ouwens, A.-H. Batens, Y. Van Nieuwenhove, B. Lapauw, Divergent
892 dynamics in systemic and tissue-specific metabolic and inflammatory responses during weight
893 loss in subjects with obesity. *Cytokine* **144**, 155587 (2021).

894 61. R. Chaleckis, I. Murakami, J. Takada, H. Kondoh, M. Yanagida, Individual variability in human
895 blood metabolites identifies age-related differences. *Proceedings of the National Academy of
896 Sciences* **113**, 4252-4259 (2016).

897 62. J. De Brandt, W. Derave, F. Vandenabeele, P. Pomiès, L. Blancquaert, C. Keytsman, M. S.
898 Barusso-Grüninger, F. F. de Lima, M. Hayot, M. A. Spruit, Efficacy of 12 weeks oral beta-alanine
899 supplementation in patients with chronic obstructive pulmonary disease: a double-blind,

900 randomized, placebo-controlled trial. *Journal of cachexia, sarcopenia and muscle* **13**, 2361-
901 2372 (2022).

902 63. L. Gliemann, N. Rytter, P. Piil, J. Nilton, T. Lind, M. Nyberg, M. Cocks, Y. Hellsten, The
903 endothelial mechanotransduction protein platelet endothelial cell adhesion molecule-1 is
904 influenced by aging and exercise training in human skeletal muscle. *Frontiers in physiology* **9**,
905 1807 (2018).

906 64. L. Gliemann, N. Rytter, A. Tamariz-Ellemann, J. Egelund, N. Brandt, H. H. Carter, Y. Hellsten,
907 Lifelong Physical Activity Determines Vascular Function in Late Postmenopausal Women.
908 *Medicine and Science in Sports and Exercise* **52**, 627-636 (2020).

909 65. L. Olsen, B. Hoier, C. Hansen, M. Leinum, H. Carter, T. Jorgensen, J. Bangsbo, Y. Hellsten,
910 Angiogenic potential is reduced in skeletal muscle of aged women. *The Journal of Physiology*
911 **598**, 5149-5164 (2020).

912 66. C. Hansen, S. Møller, T. Ehlers, K. A. Wickham, J. Bangsbo, L. Gliemann, Y. Hellsten, Redox
913 balance in human skeletal muscle-derived endothelial cells-Effect of exercise training. *Free
914 Radical Biology and Medicine* **179**, 144-155 (2022).

915 67. B. Høier, K. Olsen, M. Nyberg, J. Bangsbo, Y. Hellsten, Contraction-induced secretion of VEGF
916 from skeletal muscle cells is mediated by adenosine. *American Journal of Physiology-Heart and
917 Circulatory Physiology* **299**, H857-H862 (2010).

918 68. C. G. Perry, D. A. Kane, C.-T. Lin, R. Kozy, B. L. Cathey, D. S. Lark, C. L. Kane, P. M. Brophy, T. P.
919 Gavin, E. J. Anderson, Inhibiting myosin-ATPase reveals a dynamic range of mitochondrial
920 respiratory control in skeletal muscle. *Biochemical Journal* **437**, 215-222 (2011).

921 69. S. de Jager, S. Van Damme, S. De Baere, S. Croubels, R. Jäger, M. Purpura, E. Lievens, J. G.
922 Bourgois, W. Derave, No Effect of Acute Balenine Supplementation on Maximal and
923 Submaximal Exercise Performance in Recreational Cyclists. *International Journal of Sport
924 Nutrition and Exercise Metabolism* **1**, 1-9 (2023).

925 70. M. R. Larsen, D. E. Steenberg, J. B. Birk, K. A. Sjøberg, B. Kiens, E. A. Richter, J. F. Wojtaszewski,
926 The insulin-sensitizing effect of a single exercise bout is similar in type I and type II human
927 muscle fibres. *The Journal of Physiology* **598**, 5687-5699 (2020).

928 71. M. I. Love, W. Huber, S. Anders, Moderated estimation of fold change and dispersion for RNA-
929 seq data with DESeq2. *Genome biology* **15**, 1-21 (2014).

930

931 **Acknowledgements**

932 For human brain tissues, all material has been collected from donors for or from whom a written
933 informed consent for a brain autopsy and the use of the material and clinical information for research
934 purposes had been obtained by the Netherlands Brain Bank (NBB). The experiment protocols and
935 methods used for analysing brain samples were conducted with the approval of the NBB and the
936 Medical Ethical Committee of Hasselt University, and carried out according to institutional guidelines.
937 All HCDs analyses were performed using an UHPLC-MS/MS instrument part of the Ghent University
938 MSsmall Expertise Centre for advanced mass spectrometry analysis of small organic molecules. Also,
939 the University Biobank Limburg (UBiLim) is acknowledged for providing storage and release of some
940 human biological material used in this publication. Figure 7D, 7E, 7F and FG (experimental setups) were
941 created in BioRender. The technical assistance of Jens Jung Nielsen, Anneke Volkaert, Thomas Ehlers,
942 Nicklas Frisch and Josephine Rol is greatly appreciated.

943 **Funding**

944 Research Foundation-Flanders – FWO 11B4220N (TVDS)
945 Research Foundation-Flanders – FWO 1138520N (JS)
946 Research Foundation-Flanders – FWO 11C0421N (SDJ)
947 Research Foundation-Flanders – FWO V433222N (TVDS)
948 Research Foundation-Flanders – FWO G080321N (WD)

949 **Author contributions**

950 TVDS, JSp, SDJ and WD designed the study.
951 TVDS, JSp, SDJ, CH, JSt, BVer, CVA and MV performed the experiments and/or biochemical analyses.
952 TVDS, JSp, SDJ, JDB, RVT, KV, DH, TB, BL, CVP, KD, BVan and LG contributed to tissue collection.
953 SC, BCP, BO, LG, YH and WD supervised the study.
954 TVDS, JSp, SDJ and WD analyzed the data.
955 TVDS, JSp and WD drafted the manuscript.
956 All authors approved the final version of the manuscript.

957 **Competing interests**

958 The authors declare that they have no competing interests.

959 **Data and materials availability**

960 All data needed to evaluate the conclusions in the paper are present in the manuscript and
961 supplementary materials. Additional data related to this paper can be obtained upon reasonable
962 request to the author.